elav-GAL4/elav-GAL4 (elav>UAS-*Caz*-IR/UAS-*Caz*-IR), w; UAS-*Caz*-IR363–399/*ter94*^{K15502}; *elav-GAL4/+* (elav>UAS-*Caz*-IR/*ter94*^{K15502}), w; UAS-*Caz*-IR363–399/UAS-*GFP*; *elav-GAL4/+* (elav>UAS-*Caz*-IR/UAS-*GFP*), w; UAS-*Caz*-IR363–399/UAS-*ter94*; *elav-GAL4/+* (elav>UAS-*Caz*-IR/UAS-*ter94*).

Immunohistochemistry

Rabbit anti-Caz antibodies were raised against amino acid residues 29–45 and 383–399 of Caz and were produced previously (19). For immunohistochemical analysis, CNS tissues were dissected from third instar larvae and fixed in 4% paraformaldehyde/phosphate buffered saline (PBS) for 15 min at 25°C. These tissue samples were washed with PBS containing 0.3% Triton X-100; fixed samples were then incubated with Alexa 488-conjugated phalloidin (1 unit/200 μl) in PBS containing 0.3% Triton X-100 for 20 min at 25°C. The samples were then blocked with blocking buffer (PBS containing 0.15% Triton X-100 and 10% normal goat serum) for 30 min at 25°C, and then incubated with 1 : 1000 diluted rabbit anti-Caz antibody in the blocking buffer for 20 h at 4°C. After extensive washing with PBS containing 0.3% Triton X-100, samples were incubated in the dark with secondary antibodies labeled with Alexa 546 (1 : 400; Invitrogen) diluted in the blocking buffer for 3 h at 25°C. After washing with PBS containing 0.3% Triton X-100, the samples were stained with DAPI (0.5 μg/ml)/PBS/0.1% Triton X-100. After extensive washing with PBS containing 0.1% Triton X-100 and PBS, the samples were mounted in Vectashield (Vector Laboratories-Inc.) and observed under a confocal laser scanning microscope (OLYMPUS FLUOVIEW FV10i). Images were analyzed with the program MetaMorph Imaging System 7.7 (Molecular Devices Inc.). The use of this program made it possible to quantify the average and the standard error of fluorescence emission from nuclei of each fly strain.

For NMJ staining, third instar larvae were dissected in HL3 saline (49), and then fixed in 4% paraformaldehyde/PBS for 30 min. The blocking buffer contained 2% bovine serum albumin and 0.1% Triton X-100 in PBS. Fluorescein isothiocyanate-conjugated goat anti-horseradish peroxidase (HRP) (1:1000, MP Biochemicals) was used as the detection antibody. The samples were mounted and observed under a confocal laser scanning microscope (Carl Zeiss LSM510, Jena, Germany). MN 4 (Ib) in muscle 4 in abdominal segment 2 was quantified. Images were acquired using a Zeiss LSM 510 confocal laser scanning microscope by merging 1 μm interval z-sections onto a single plane. The MetaMorph imaging system was used to measure nerve terminal branch lengths and Ib bouton sizes.

Immunoblotting analysis

Protein extracts from the CNS of *Drosophila* carrying *elav/+*, elav>UAS-*Caz*-IR, elav>UAS-*Caz*-IR/*ter94* ^{K15502}, elav>UAS-*Caz*-IR/UAS-*GFP* and elav>UAS-*Caz*-IR/UAS-*ter94* larvae were prepared as described previously (19). Briefly, the CNS was excised from third instar larvae and homogenized in a sample buffer containing 50 mM Tris–HCl (pH 6.8), 2% sodium dodecyl sulfate (SDS), 10% glycerol, 0.1% bromophenol blue and 1.2% β-mercaptoethanol. The homogenates were boiled at 100°C for 5 min and then centrifuged. The supernatants (extracts) were electrophoretically separated on SDS-polyacrylamide gels containing 12% acrylamide and then transferred to polyvinylidene difluoride membranes (Merck, Millipore, MA, USA). The blotted membranes were blocked with tris-buffered saline/0.05% Tween containing 5% skim milk for 1 h at 25°C, followed by incubation with rabbit polyclonal anti-Caz at a 1:5000 dilution for 16 h at 4°C. After washing, the membranes were incubated with HRP-conjugated anti-rabbit IgG (Thermo Scientific, IL, USA) at 1:10 000 dilution for 2 h at 25°C. Antibody binding was detected using ECL Western blotting detection reagents (Thermo Scientific) and images were analyzed using an ImageQuant^{TM} LAS 4000 image analyzer (GE Healthcare Bioscience, Tokyo, Japan). To compare Caz protein levels in the CNS extracts of those larvae, densitometric quantification of the 45-kDa Caz protein bands was carried out. The relative band intensities were quantified and normalized to Coomassie Brilliant Blue staining, then expressed as the percentage of the band intensity derived from larvae carrying *elav/+*.

Scanning electron microscopy

Adult flies were anesthetized with 99% diethyl ether, mounted on stages and observed under an SEM V-7800 (Keyence Inc.) in the low vacuum mode (50). In every experiment, at least five adult flies were chosen from each line for scanning electron microscopy to assess the eye phenotype. For each experiment, there was no significant variation in eye phenotype among the five individuals from the same strain.

Longevity assay

Longevity assays were carried out in a humidified, temperature-controlled incubator set at 25°C and 60% humidity on a 12-h light and 12-h dark cycle; flies were maintained on standard fly food. Flies carrying *elav/+* ($n = 151$), elav>UAS-*Caz*-IR ($n = 123$), elav>UAS-*Caz*-IR/*ter94*^{K15502} ($n = 120$), elav>UAS-*Caz*-IR/UAS-*GFP* ($n = 140$) or elav>UAS-*Caz*-IR/UAS-*ter94* ($n = 140$) were placed at 28°C, and newly eclosed adult male flies were separated and placed in vials at a low density (20 flies per vial). Every 3 days, they were transferred to new tubes containing fresh food and deaths were scored. The survival rate was determined by plotting a graph of the percentage of surviving flies among total flies at the starting point of each experiment versus days.

Climbing assay

Climbing assays were performed as described previously (29). Flies carrying *elav/+*, UAS-*Caz*-IR/+, *ter94*^{K15502}/+, elav>UAS-*Caz*-IR, elav>UAS-*Caz*-IR/*ter94*^{K15502}, elav>UAS-*Caz*-IR/UAS-*GFP* and elav>UAS-*Caz*-IR/UAS-*ter94* were placed at 28°C, and newly eclosed adult male flies were separated and placed in vials at a density of 20 flies per vial. Flies were transferred, without anesthesia, to a conical tube. The tubes were tapped to collect the flies to the bottom, and they were then given 30 s to climb the wall. After 30 s, the flies were collected at the bottom by tapping of the tube and were again allowed to climb for 30 s. Similar procedures, all of which were videotaped, were repeated five times in total. For each climbing experiment, the height to which each fly

climbed was scored as score (height climbed); 0 (less than 2 cm), 1 (between 2 and 3.9 cm), 2 (between 4 and 5.9 cm), 3 (between 6 and 7.9 cm), 4 (between 8 and 9.9 cm) or 5 (greater than 10 cm). The climbing index for each fly strain was calculated as follows; each score was multiplied by the number of flies for which that score was recorded, and the products were summed up, then divided by five times the total number of flies examined. These climbing assays were carried out every 7 days until the 28th day after eclosion.

Data analysis

GraphPad Prism version 6.0 was used to perform each statistical analysis. The Mann–Whiney test was used for the assessment of the statistical significance of comparisons between two groups of data. For other assays, one-way analysis of variance (ANOVA) was used to determine the statistical significance of comparisons between groups of data. When the two-way ANOVA showed significant variation among groups, a subsequent Dunnett's test was used for pairwise comparisons between groups. All data are shown as mean ± standard error (SE).

SUPPLEMENTARY MATERIAL

Supplementary Material is available at *HMG* online.

ACKNOWLEDGEMENTS

We would like to thank Dr Kakizuka for generously providing us the UAS-*ter94* fly strains used in these experiments. We would also like to acknowledge Dr H. Yoshida, Ms R. Sahashi, Mr K. Morishita and Mr K. Shimaji for valuable discussion, technical support and suggestions. We thank the Bloomington *Drosophila* stock center, the Vienna *Drosophila* RNAi center and Kyoto *Drosophila* Genetic Resource Center for giving us fly lines.

Conflict of Interest statement. None declared.

FUNDING

This work was supported by Grants-in-Aid from the Research Committee of CNS. Degenerative Diseases, the Ministry of Health, Labour and Welfare of Japan (T.T.), and partly supported by "Integrated Research on Neuropsychiatric Disorders" carried out under the Strategic Research Program for Brain Sciences by the Ministry of Education, Culture, Sports, Science and Technology of Japan (Y.N.). The funders had no role in study design, data collection and analysis, decision to publish or preparation of the manuscript.

REFERENCES

1. Boillée, S., Vande Velde, C. and Cleveland, D.W. (2006) ALS: a disease of motor neurons and their nonneuronal neighbors. *Neuron*, **52**, 39–59.
2. Mackenzie, I.R., Rademakers, R. and Neumann, M. (2010) TDP-43 and FUS in amyotrophic lateral sclerosis and frontotemporal dementia. *Lancet Neurol.*, **9**, 995–1007.
3. Lomen-Hoerth, C., Anderson, T. and Miller, B. (2002) The overlap of amyotrophic lateral sclerosis and frontotemporal dementia. *Neurology*, **59**, 1077–1079.
4. Murphy, J.M., Henry, R.G., Langmore, S., Kramer, J.H., Miller, B.L. and Lomen-Hoerth, C. (2007) Continuum of frontal lobe impairment in amyotrophic lateral sclerosis. *Arch. Neurol.*, **64**, 530–534.
5. Dormann, D. and Haass, C. (2013) Fused in sarcoma (FUS): an oncogene goes awry in neurodegeneration. *Mol. Cell Neurosci.*, **56**, 475–486.
6. Lemmens, R., Moore, M.J., Al-Chalabi, A., Brown, R.H. Jr. and Robberecht, W. (2010) RNA metabolism and the pathogenesis of motor neuron diseases. *Trends Neurosci.*, **33**, 249–258.
7. Gitcho, M.A., Baloh, R.H., Chakraverty, S., Mayo, K., Norton, J.B., Levitch, D., Hatanpaa, K.J., White, C.L. 3rd., Bigio, E.H., Caselli, R. *et al.* (2008) TDP-43 A315 T mutation in familial motor neuron disease. *Ann. Neurol.*, **63**, 535–538.
8. Yokoseki, A., Shiga, A., Tan, C.F., Tagawa, A., Kaneko, H., Koyama, A., Eguchi, H., Tsujino, A., Ikeuchi, T., Kakita, A. *et al.* (2008) TDP-43 mutation in familial amyotrophic lateral sclerosis. *Ann. Neurol.*, **63**, 538–542.
9. Kabashi, E., Valdmanis, P.N., Dion, P., Spiegelman, D., McConkey, B.J., Vande Velde, C., Bouchard, J.P., Lacomblez, L., Pochigaeva, K., Salachas, F. *et al.* (2008) TARDBP mutations in individuals with sporadic and familial amyotrophic lateral sclerosis. *Nat. Genet.*, **40**, 572–574.
10. Sreedharan, J., Blair, I.P., Tripathi, V.B., Hu, X., Vance, C., Rogelj, B., Ackerley, S., Durnall, J.C., Williams, K.L., Buratti, E. *et al.* (2008) TDP-43 mutations in familial and sporadic amyotrophic lateral sclerosis. *Science*, **319**, 1668–1672.
11. Pesiridis, G.S., Lee, V.M. and Trojanowski, J.Q. (2009) Mutations in TDP-43 link glycine-rich domain functions to amyotrophic lateral sclerosis. *Hum. Mol. Genet.*, **18**, R156–R162.
12. Kwiatkowski, T.J. Jr., Bosco, D.A., Leclerc, A.L., Tamrazian, E., Vanderburg, C.R., Russ, C., Davis, A., Gilchrist, J., Kasarskis, E.J., Munsat, T. *et al.* (2009) Mutations in the FUS/TLS gene on chromosome 16 cause familial amyotrophic lateral sclerosis. *Science*, **323**, 1205–1208.
13. Vance, C., Rogelj, B., Hortobágyi, T., De, Vos, K.J., Nishimura, A.L., Sreedharan, J., Hu, X., Smith, B., Ruddy, D., Wright, P. *et al.* (2009) Mutations in FUS, an RNA processing protein, cause familial amyotrophic lateral sclerosis type 6. *Science*, **323**, 1208–1211.
14. Hewitt, C., Kirby, J., Highley, J.R., Hartley, J.A., Hibberd, R., Hollinger, H.C., Williams, T.L., Ince, P.G., McDermott, C.J. and Shaw, P.J. (2010) Novel FUS/TLS mutations and pathology in familial and sporadic amyotrophic lateral sclerosis. *Arch. Neurol.*, **67**, 455–461.
15. Rademakers, R., Stewart, H., Dejesus-Hernandez, M., Krieger, C., Graff-Radford, N., Fabros, M., Briemberg, H., Cashman, N., Eisen, A. and Mackenzie, I.R. (2010) Fus gene mutations in familial and sporadic amyotrophic lateral sclerosis. *Muscle Nerve*, **42**, 170–176.
16. Zinszner, H., Sok, J., Immanuel, D., Yin, Y. and Ron, D. (1997) TLS (FUS) binds RNA in vivo and engages in nucleo-cytoplasmic shuttling. *J. Cell Sci.*, **110**, 1741–1750.
17. Lagier-Tourenne, C., Polymenidou, M. and Cleveland, D.W. (2010) TDP-43 and FUS/TLS: emerging roles in RNA processing and neurodegeneration. *Hum. Mol. Genet.*, **19**, R46–R64.
18. Feiguin, F., Godena, V.K., Romano, G., D'Ambrogio, A., Klima, R. and Baralle, F.E. (2009) Depletion of TDP-43 affects *Drosophila* motoneurons terminal synapsis and locomotive behavior. *FEBS Lett.*, **583**, 1586–1592.
19. Sasayama, H., Shimamura, M., Tokuda, T., Azuma, Y., Yoshida, T., Mizuno, T., Nakagawa, M., Fujikake, N., Nagai, Y. and Yamaguchi, M. (2012) Knockdown of the *Drosophila* fused in sarcoma (FUS) homologue causes deficient locomotive behavior and shortening of motoneuron terminal branches. *PLoS One*, 7, e39483.
20. Kabashi, E., Bercier, V., Lissouba, A., Liao, M., Brustein, E., Rouleau, G.A. and Drapeau, P. (2011) FUS and TARDBP but not SOD1 interact in genetic models of amyotrophic lateral sclerosis. *PLoS Genet.*, 7, e1002214.
21. Wang, J.W., Brent, J.R., Tomlinson, A., Shneider, N.A. and McCabe, B.D. (2011) The ALS-associated proteins FUS and TDP-43 function together to affect *Drosophila* locomotion and life span. *J. Clin. Invest.*, **121**, 4118–4126.
22. Meyer, H., Bug, M. and Bremer, S. (2012) Emerging functions of the VCP/p97 AAA-ATPase in the ubiquitin system. *Nat. Cell Biol.*, **14**, 117–123.
23. Braun, R.J. and Zischka, H. (2008) Mechanisms of Cdc48/VCP-mediated cell death: from yeast apoptosis to human disease. *Biochim. Biophys. Acta*, **1783**, 1418–1435.

24. Ritson, G.P., Custer, S.K., Freibaum, B.D., Guinto, J.B., Geffel, D., Moore, J., Tang, W., Winton, M.J., Neumann, M., Trojanowski, J.Q. *et al.* (2010) TDP-43 mediates degeneration in a novel *Drosophila* model of disease caused by mutations in VCP/p97. *J. Neurosci.*, **30**, 7729–7739.
25. Watts, G.D., Wymer, J., Kovach, M.J., Mehta, S.G., Mumm, S., Darvish, D., Pestronk, A., Whyte, M.P. and Kimonis, V.E. (2004) Inclusion body myopathy associated with Paget disease of bone and frontotemporal dementia is caused by mutant valosin-containing protein. *Nat. Genet.*, **36**, 377–381.
26. Johnson, J.O., Mandrioli, J., Benatar, M., Abramzon, Y., Van, Deerlin, V.M., Trojanowski, J.Q., Gibbs, J.R., Brunetti, M., Gronka, S., Wuu, J. *et al.* (2010) Exome sequencing reveals VCP mutations as a cause of familial ALS. *Neuron*, **68**, 857–864.
27. Stolow, D.T. and Haynes, S.R. (1995) Cabeza, a *Drosophila* gene encoding a novel RNA binding protein, shares homology with EWS and TLS, two genes involved in human sarcoma formation. *Nucleic Acids Res.*, **23**, 835–843.
28. Ruden, D.M., Sollars, V., Wang, X., Mori, D., Alterman, M. and Lu, X. (2000) Membrane fusion proteins are required for oskar mRNA localization in the *Drosophila* egg chamber. *Dev. Biol.*, **218**, 314–325.
29. Shcherbata, H.R., Yatsenko, A.S., Patterson, L., Sood, V.D., Nudel, U., Yaffe, D., Baker, D. and Ruohola-Baker, H. (2007) Dissecting muscle and neuronal disorders in a *Drosophila* model of muscular dystrophy. *EMBO J.*, **26**, 481–493.
30. Chang, H.C., Dimlich, D.N., Yokokura, T., Mukherjee, A., Kankel, M.W., Sen, A., Sridhar, V., Fulga, T.A., Hart, A.C., Van Vactor, D. *et al.* (2008) Modeling spinal muscular atrophy in *Drosophila*. *PLoS One*, **3**, e3209.
31. Chee, F., Mudher, A., Newman, T.A., Cuttle, M., Lovestone, S. and Shepherd, D. (2006) Overexpression of tau results in defective synaptic transmission in *Drosophila* neuromuscular junctions. Biochem. Soc. Trans., **34**, 88–90.
32. Hirabayashi, M., Inoue, K., Tanaka, K., Nakadate, K., Ohsawa, Y., Kamei, Y., Popiel, A.H., Sinohara, A., Iwamatsu, A., Kimura, Y. *et al.* (2001) VCP/p97 in abnormal protein aggregates, cytoplasmic vacuoles, and cell death, phenotypes relevant to neurodegeneration. *Cell Death Differ.*, **8**, 977–984.
33. Fujita, K., Nakamura, Y., Oka, T., Ito, H., Tamura, T., Tagawa, K., Sasabe, T., Katsuta, A., Motoki, K., Shiwaku, H. *et al.* (2013) A functional deficiency of TERA/VCP/p97 contributes to impaired DNA repair in multiple polyglutamine diseases. *Nat. Commun.*, **4**, 1816. doi:10.1038/ncomms2828.
34. Higashiyama, H., Hirose, F., Yamaguchi, M., Inoue, Y.H., Fujikake, N., Matsukage, A. and Kakizuka, A. (2002) Identification of ter94, *Drosophila* VCP, as a modulator of polyglutamine-induced neurodegeneration. *Cell Death Differ.*, **9**, 264–273.
35. Ishigaki, S., Hishikawa, N., Niwa, J., Iemura, S., Natsume, T., Hori, S., Kakizuka, A., Tanaka, K. and Sobue, G. (2004) Physical and functional interaction between Dorfin and Valosin-containing protein that are colocalized in ubiquitylated inclusions in neurodegenerative disorders. *J. Biol. Chem.*, **279**, 51376–51385.
36. Kakizuka, A. (2008) Roles of VCP in human neurodegenerative disorders. *Biochem. Soc. Trans.*, **36**, 105–108.
37. Mizuno, Y., Hori, S., Kakizuka, A. and Okamoto, K. (2003) Vacuole-creating protein in neurodegenerative diseases in humans. *Neurosci. Lett.*, **343**, 77–80.
38. Marti, F. and King, P.D. (2005) The p95–100 kDa ligand of the T cell-specific adaptor (TSAd) protein Src-homology-2 (SH2) domain implicated in TSAd nuclear import is p97 Valosin-containing protein (VCP). *Immunol. Lett.*, **97**, 235–243.
39. Ju, J.S. and Weihl, C.C. (2010) p97/VCP at the intersection of the autophagy and the ubiquitin proteasome system. *Autophagy*, **6**, 283–285.
40. Ling, S.C., Albuquerque, C.P., Han, J.S., Lagier-Tourenne, C., Tokunaga, S., Zhou, H. and Cleveland, D.W. (2010) ALS-associated mutations in TDP-43 increase its stability and promote TDP-43 complexes with FUS/TLS. *Proc. Natl Acad. Sci. USA*, **107**, 13318–13323.
41. van Blitterswijk, M. and Landers, J.E. (2010) RNA processing pathways in amyotrophic lateral sclerosis. *Neurogenetics*, **11**, 275–290.
42. Kim, S.H., Shanware, N.P., Bowler, M.J. and Tibbetts, R.S. (2010) Amyotrophic lateral sclerosis-associated proteins TDP-43 and FUS/TLS function in a common biochemical complex to co-regulate HDAC6 mRNA. *J. Biol. Chem.*, **285**, 34097–34105.
43. Fiesel, F.C. and Kahle, P.J. (2011) TDP-43 and FUS/TLS: cellular functions and implications for neurodegeneration. *FEBS J.*, **278**, 3550–3568.
44. Ayala, Y.M., Zago, P., D'Ambrogio, A., Xu, Y.F., Petrucelli, L., Buratti, E. and Baralle, F.E. (2008) Structural determinants of the cellular localization and shuttling of TDP-43. *J. Cell Sci.*, **121**, 3778–3785.
45. Nagai, R., Hashimoto, R. and Yamaguchi, M. (2010) *Drosophila* Syntrophins are involved in locomotion and regulation of synaptic morphology. *Exp. Cell Res.*, **316**, 2313–2321.
46. Fernández-Sáiz, V. and Buchberger, A. (2010) Imbalances in p97 co-factor interactions in human proteinopathy. *EMBO Rep.*, **11**, 479–485.
47. Manno, A., Noguchi, M., Fukushi, J., Motohashi, Y. and Kakizuka, A. (2010) Enhanced ATPase activities as a primary defect of mutant valosin-containing proteins that cause inclusion body myopathy associated with Paget disease of bone and frontotemporal dementia. *Genes Cells*, **15**, 911–922.
48. Takahashi, Y., Hirose, F., Matsukage, A. and Yamaguchi, M. (1999) Identification of three conserved regions in the DREF transcription factors from *Drosophila melanogaster* and *Drosophila virilis*. *Nucleic Acids Res.*, **27**, 510–516.
49. Stewart, B.A., Atwood, H.L., Renger, J.J., Wang, J. and Wu, C.F. (1994) Improved stability of *Drosophila* larval neuromuscular preparations in haemolymph-like physiological solutions. *J. Comp. Physiol. A*, **175**, 179–191.
50. Ly, L.L., Suyari, O., Yoshioka, Y., Tue, N.T., Yoshida, H. and Yamaguchi, M. (2013) dNF-YB plays dual roles in cell death and cell differentiation during *Drosophila* eye development. *Gene*, **520**, 106–118.

Supplementary Materials

Supplementary Figure 1. Immunoblotting analysis of the CNS extracts of third instar larvae. (A) A representative result of the analysis of protein extracts from the CNS of the *elav/+,* elav>UAS-*Caz*-IR, elav>UAS-*Caz*-IR/*ter94*^{K15502}, elav>UAS-*Caz*-IR/UAS-*GFP* and elav>UAS-*Caz*-IR/UAS-*ter94* larvae (n = 5, each). The blots are probed with the polyclonal anti-Caz antibody used in the previous study (19). A 45-kDa band (arrow) corresponds to the Caz protein. (B) Densitometric quantification of the 45-kDa bands in each fly strain used in (A). The intensity of the 45-kDa band which indicates the expression level of Caz protein is much weaker in larvae carrying elav>UAS-*Caz*-IR than in the larvae carrying *elav/+*. Besides, there is no apparent difference in the intensity of the Caz protein band between the larvae carrying elav>UAS-*Caz*-IR and elav>UAS-*Caz*-IR/*ter94*^{K15502}. Similarly, there is no apparent difference in the intensity of the band between the larvae carrying elav>UAS-*Caz*-IR/UAS-*GFP* and elav>UAS-*Caz*-IR/UAS-*ter94*.

Supplementary Figure 2. The locomotive ability of each control flies, which carry *elav/+* (a driver control, n = 255), UAS-*Caz*-IR/+ (a responder control, n = 250), *ter94*^{k15502}/+ (n = 235). There are no significant differences in climbing abilities among those fly lines in each day after eclosion that was monitored until 14 days.

Supplementary Figure 3. Life-span analyses of flies of each genotype. Percentage survival of adult male flies of the indicated genotype is shown. (A) There are no significant differences in life spans among the control flies carrying *elav/+* (n = 151), neuron-specific *Caz*-knockdown flies carrying elav>UAS-*Caz*-IR (n = 123), and flies

carrying elav>UAS-*Caz*-IR/*ter94*^{K15502} (n = 120). (B) Similarly, there are no significant differences in life spans between flies carrying elav>UAS-*Caz*-IR/UAS-*GFP* (n = 140) and those carrying elav>UAS-*Caz*-IR/UAS-*ter94* (n = 140).

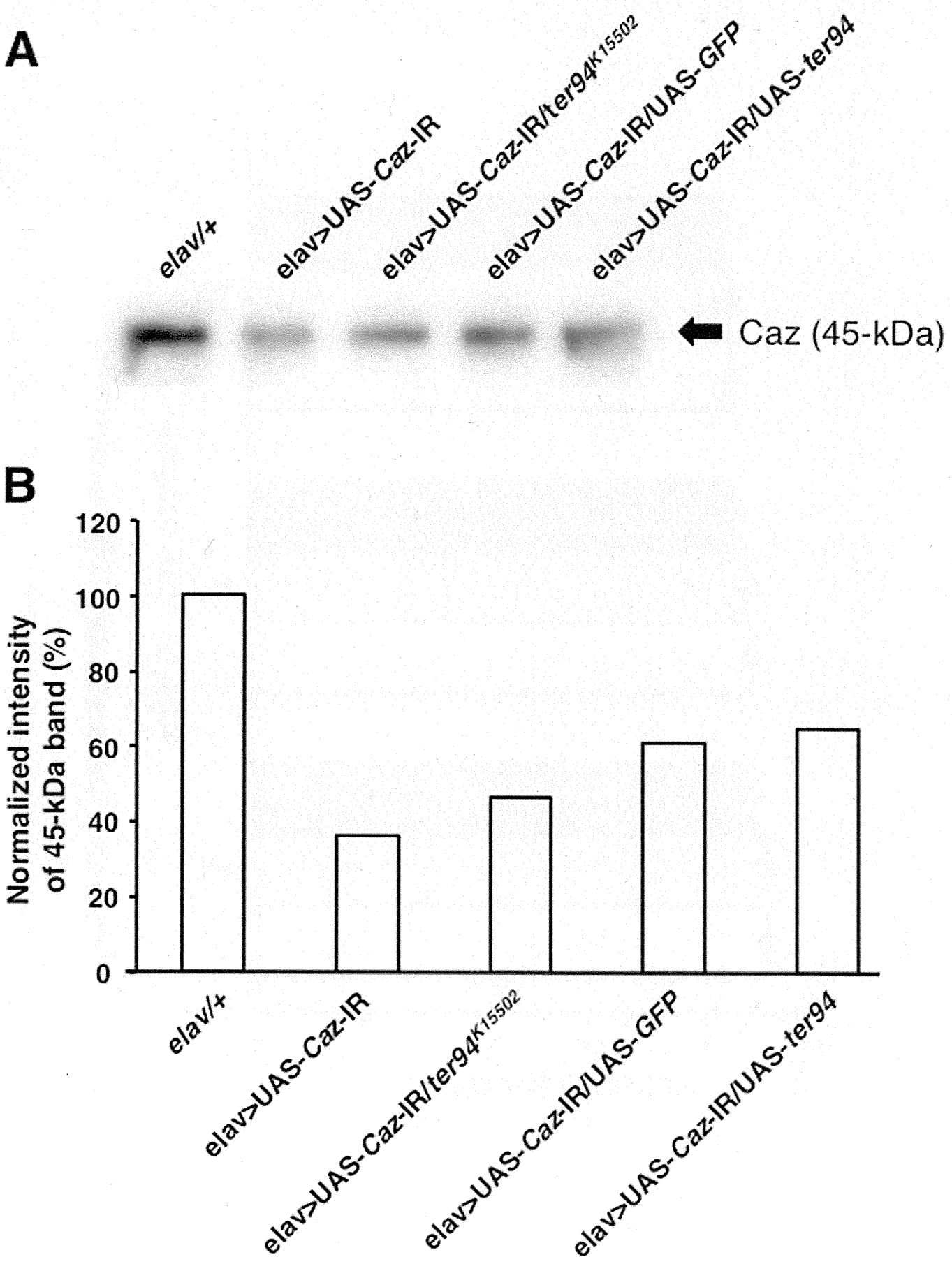
A
elav/+
elav>UAS-Caz-IR
elav>UAS-Caz-IR/ter94K15502
elav>UAS-Caz-IR/UAS-GFP
elav>UAS-Caz-IR/UAS-ter94
Caz (45-kDa)
B
Normalized intensity of 45-kDa band (%)
120
100
80
60
40
20
0
elav/+
elav>UAS-Caz-IR
elav>UAS-Caz-IR/ter94K15502
elav>UAS-Caz-IR/UAS-GFP
elav>UAS-Caz-IR/UAS-ter94

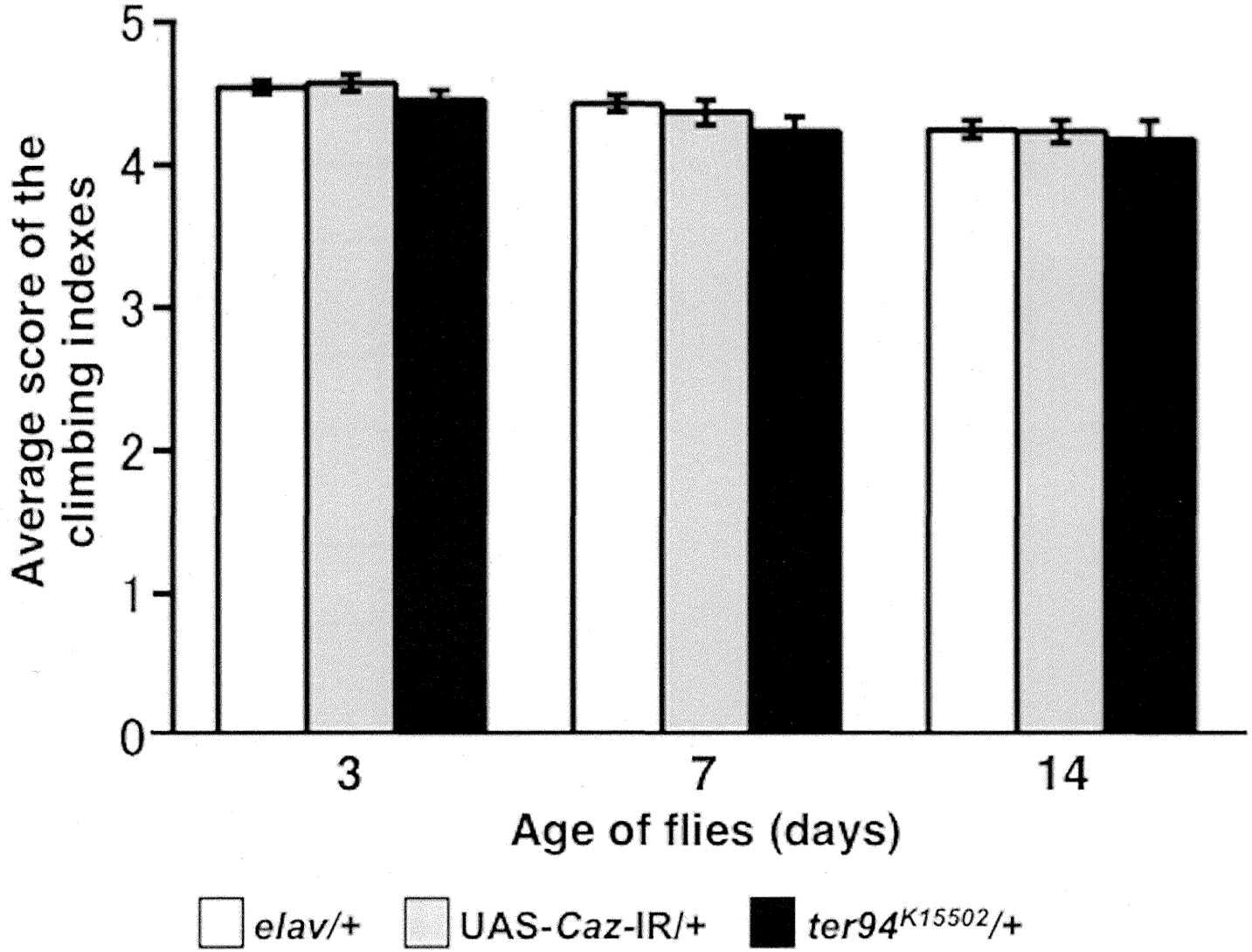
Average score of the climbing indexes
5
4
3
2
1
0
3
7
14
Age of flies (days)
elav/+
UAS-Caz-IR/+
ter94K15502/+

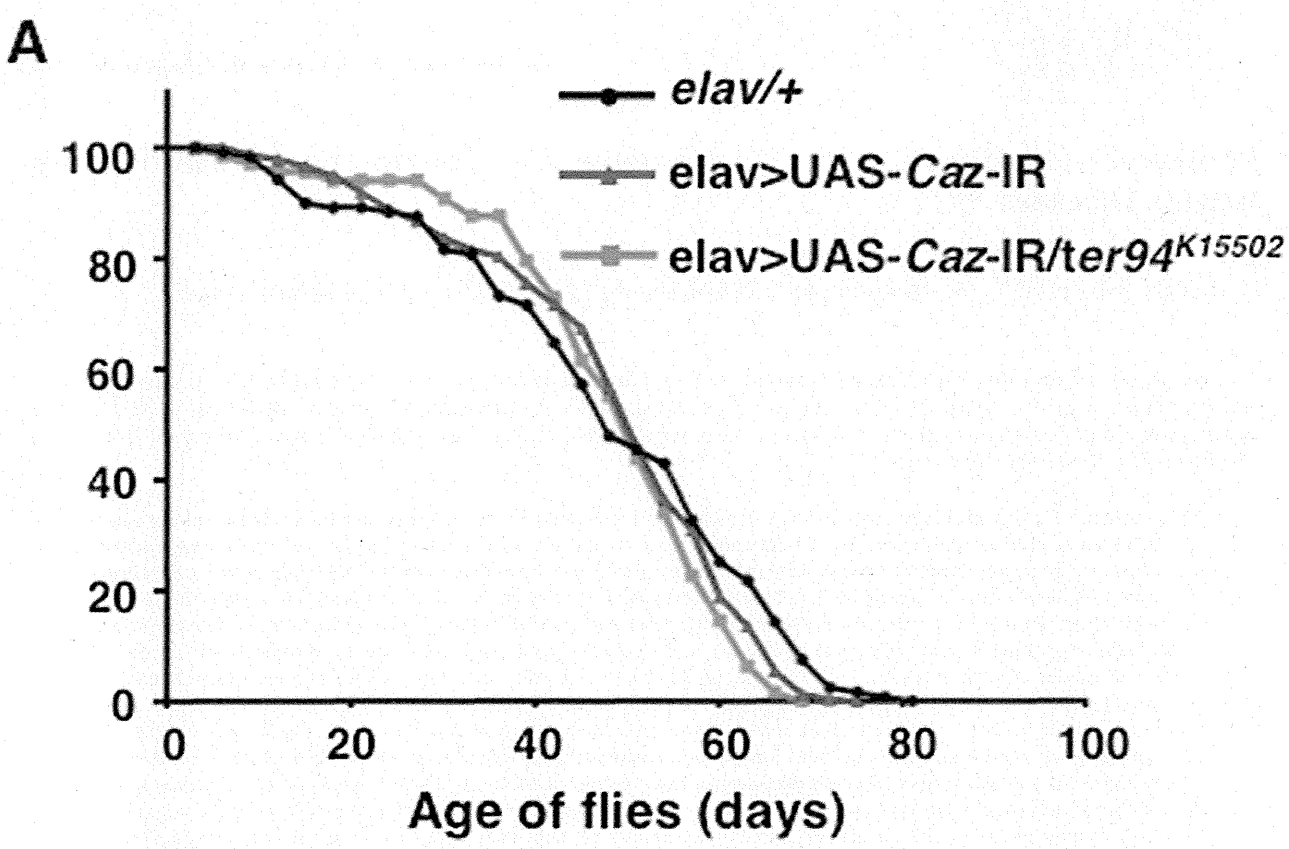
A
elav/+
elav>UAS-Caz-IR
elav>UAS-Caz-IR/ter94K15502
100
80
60
40
20
0
0
20
40
60
80
100
Age of flies (days)

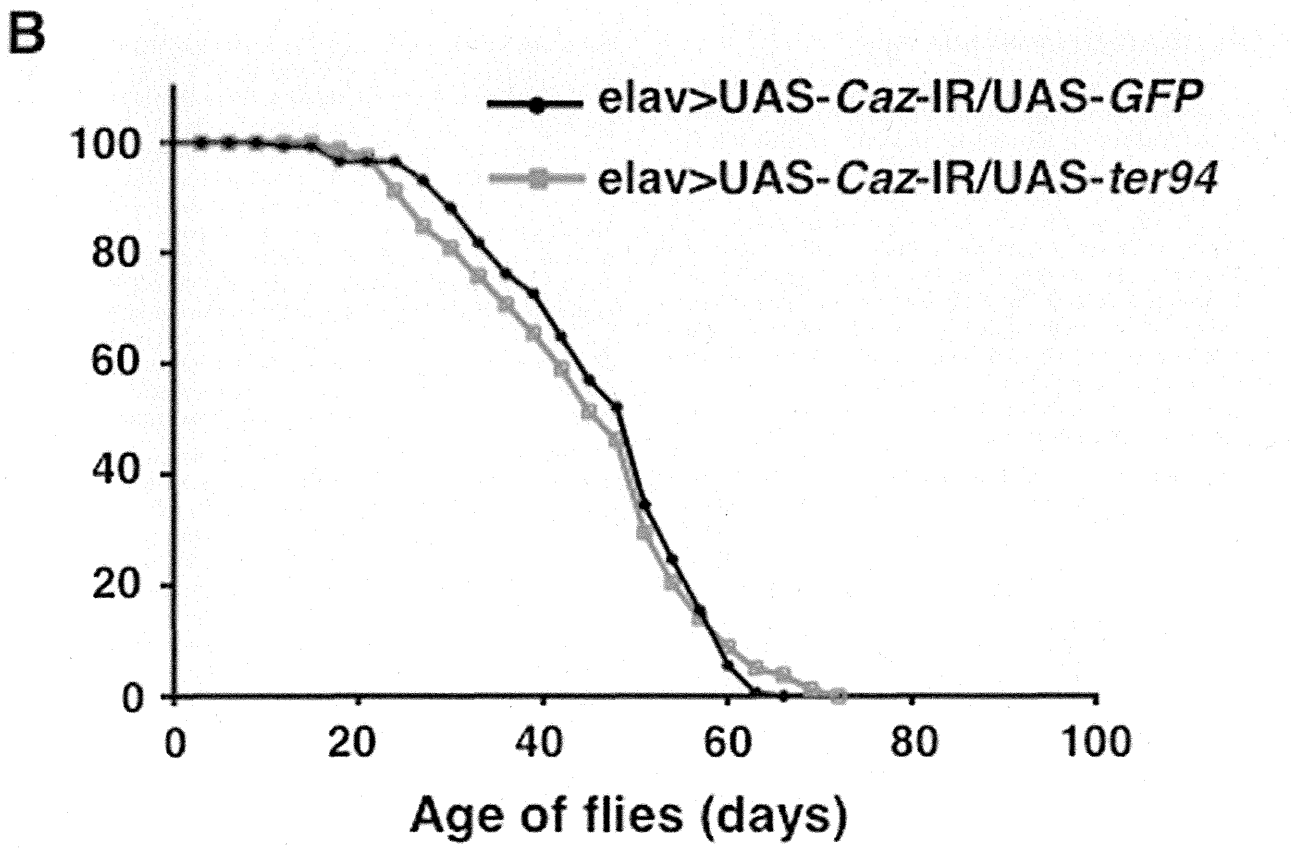
B
elav>UAS-Caz-IR/UAS-GFP
elav>UAS-Caz-IR/UAS-ter94
100
80
60
40
20
0
0
20
40
60
80
100
Age of flies (days)

FINAL

Send Orders for Reprints to reprints@benthamscience.net

Current Medicinal Chemistry, 2014, *21*, ????-????

Peptide-Based Therapeutic Approaches for Treatment of the Polyglutamine Diseases

Toshihide Takeuchi[1,3,*], H. Akiko Popiel[1], Shiroh Futaki[3], Keiji Wada[1], and Yoshitaka Nagai[1,2,*]

[1]*Department of Degenerative Neurological Diseases, National Institute of Neuroscience, National Center of Neurology and Psychiatry, Kodaira, Tokyo 187-8502, Japan;* [2]*Core Research for Evolutional Science and Technology (CREST), Japan Science and Technology Agency, Kawaguchi, Saitama 332-0012, Japan;* [3]*Institute for Chemical Research, Kyoto University, Uji, Kyoto 611-0011, Japan*

Abstract: The polyglutamine (polyQ) diseases including Huntington's disease and spinocerebellar ataxias are a group of inherited neurodegenerative diseases that are caused by an abnormal expansion of the polyQ stretch in disease-causative proteins. The expanded polyQ stretches are intrinsically unstable and are prone to form insoluble aggregates and inclusion bodies. Recent studies have revealed that the expanded polyQ proteins gain cytotoxicity during the aggregation process, which may possibly cause detrimental effects on a wide range of essential cellular functions leading to eventual neuronal degeneration. Based on the pathogenic mechanism of the polyQ diseases, several therapeutic approaches have been proposed to date. Among them, here we focus on peptide-based approaches that target either aggregate formation of the polyQ proteins or abnormal cellular processes induced by the expanded polyQ proteins. Although both approaches are effective in suppressing cytotoxicity of the abnormal polyQ proteins and the disease phenotypes of animal models, the former approach is more attractive since it targets the most upstream change occurring in the polyQ diseases, and is therefore expected to be effective against various downstream functional abnormalities in a broad range of polyQ diseases. One of the major current problems that must be overcome for development of peptide-based therapies of the polyQ diseases is the issue of brain delivery, which is also discussed in this article. We hope that in the near future effective therapies are developed, and bring hope to many patients suffering from the currently untreatable polyQ diseases.

Keywords: Neurodegeneration, peptide, polyglutamine diseases, protein aggregation, therapy.

THE POLYGLUTAMINE DISEASES

The polyglutamine (polyQ) diseases are a group of inherited neurodegenerative disorders characterized by a common genetic mutation in the coding sequence of each disease-causative gene, in which a trinucleotide CAG repeat encoding a polyQ stretch is abnormally expanded (>35-40 repeats) [1-3]. So far, nine disorders have been recognized as such diseases, including Huntington's disease (HD), spinal and bulbar muscular atrophy (SBMA), several types of spinocerebeller ataxias (SCAs) [2]. These diseases are all characterized by the progressive degeneration and loss of neurons in various regions of the brain, resulting in progressive neurological and psychiatric symptoms such as cognitive impairment and motor disturbance. No effective treatment for the polyQ diseases has been established to date.

The molecular basis of the polyQ diseases is the abnormal expansion of a polyQ stretch in each host protein. In most cases, the threshold polyQ length for disease manifestation is around 35-40 repeats, as polyQ expansions longer than 40 repeats typically result in the polyQ diseases [3]. For example, the polyQ length in huntingtin (Htt), the causative protein of HD, ranges in size from 5 to 35 repeats in normal subjects, but is expanded to more than 40 repeats in patients with HD [4]. The polyQ length in the disease-causative protein can also affect the disease progression, as it correlates tightly with the age at onset and severity of disease [5, 6]. Animal studies have demonstrated that typical disease phenotypes such as progressive degeneration and loss of neurons in the brain can be caused by expression of the expanded polyQ stretch alone, further supporting the pathological importance of the abnormal expansion of the polyQ stretch [7-11]. These facts strongly indicate that the polyQ diseases are caused by a gain of toxic function mechanism of the expanded polyQ stretch, and are considered to be unrelated with the specific functions of each host protein.

The expanded polyQ stretches are intrinsically unstable, and are likely to form insoluble aggregates and inclusion bodies, which are a common pathological characteristic observed in the brain of polyQ disease patients as well as animal models [12, 13]. The mechanisms as to how expanded polyQ proteins form aggregates and the relationship between aggregate formation and cytotoxicity have been extensively studied [14-18]. Recent accumulating evidence strongly indicate that abnormal intermediate species such as oligomeric intermediates and even misfolded monomers of the expanded polyQ proteins which form prior to aggregates/inclusion bodies could be more toxic to neurons compared with in-

*Address correspondence to this author at the Department of Degenerative Neurological Diseases, National Institute of Neuroscience, National Center of Neurology and Psychiatry, 4-1-1 Ogawa-Higashi, Kodaira, Tokyo 187-8502, Japan; Tels: +81-42-346-1715 and +81-774-38-3211;
Faxes: +81-42-346-1745 and +81-774-32-3038;
E-mails: nagai@ncnp.go.jp and takeuchi@scl.kyoto-u.ac.jp

0929-8673/14 $58.00+.00

soluble aggregates/inclusion bodies [19-23]. Although it is still unclear which intermediate species are responsible for polyQ disease pathogenesis, these facts indicate that the expanded polyQ protein gains cytotoxicity during the aggregation process.

THERAPEUTIC APPROACHES FOR THE POLYGLUTAMINE DISEASES

Since proteins with an abnormally expanded polyQ stretch gain cytotoxicity during their aggregation process, suppression of misfolding and aggregate formation could be a potential therapeutic approach for treatment of the polyQ diseases [3]. Several studies have actually demonstrated in polyQ disease models that increasing levels of molecular chaperones [24-28] and expression of intracellular antibodies (intrabodies) [29-31] successfully reduce the eventual toxicity in neurons through suppression of polyQ protein accumulation and inclusion body formation [32, 33]. Small molecules [34-38] and peptides [39-41] that interfere with the aggregation process of the expanded polyQ protein were also shown to suppress polyQ-induced neurodegeneration in cell culture and animal models of the polyQ diseases. In addition, activation of protein degradation systems, which accelerate the clearance of the polyQ proteins, has been shown to be quite effective to suppress aggregate formation and eventual cell death [42,43]. Since suppression of polyQ aggregation is expected to broadly correct the functional abnormalities of multiple downstream cellular processes (see below), misfolding and aggregate formation of the expanded polyQ proteins are one of the most ideal therapeutic targets of the polyQ diseases [3] (Fig. **1**).

On the other hand, it is well known that polyQ disease patients as well as animal models exhibit dysfunctions in various cellular processes in the cascade of polyQ pathogenesis. This includes abnormalities in essential cellular functions including transcription [44], proteasomal degradation [45], synaptic transmission [46], axonal transport [47] and Ca^{2+} signaling pathways [48], which probably contribute to neuronal dysfunction and eventual loss of neurons in various regions of the brain [12, 49, 50]. Although the exact mechanisms as to how they eventually cause degeneration of neurons in patients of the polyQ diseases have not yet been clarified, these cellular processes that are thought to be eventually impaired in the pathogenic cascade are also potential therapeutic targets for treatment of the polyQ diseases (Fig. **1**).

In the following sections, selected examples of peptide-based therapeutic approaches focusing on these targets are introduced (Table **1**), and the current problems that must be overcome for the development of peptide-based therapies for the polyQ diseases are discussed.

PEPTIDE-BASED INHIBITORS OF POLYGLUTAMINE AGGREGATION

Therapeutic approaches targeting the polyQ stretch are particularly attractive because effective inhibitors would be expected to work generally on a broad spectrum of the polyQ diseases. Trottier *et al.* showed that the anti-polyQ monoclonal antibody 1C2 binds preferentially to longer polyQ repeats compared with short repeats [51]. Similar preferential binding to expanded polyQ proteins has been reported for the monoclonal antibodies MW1 [52] and 3B5H10 [53]. These studies led to the idea that expanded polyQ stretches may possess structurally different conformations from the shorter ones, and that potential molecules that specifically recognize and bind to such abnormal conformations could interfere with the aggregation processes of expanded polyQ proteins.

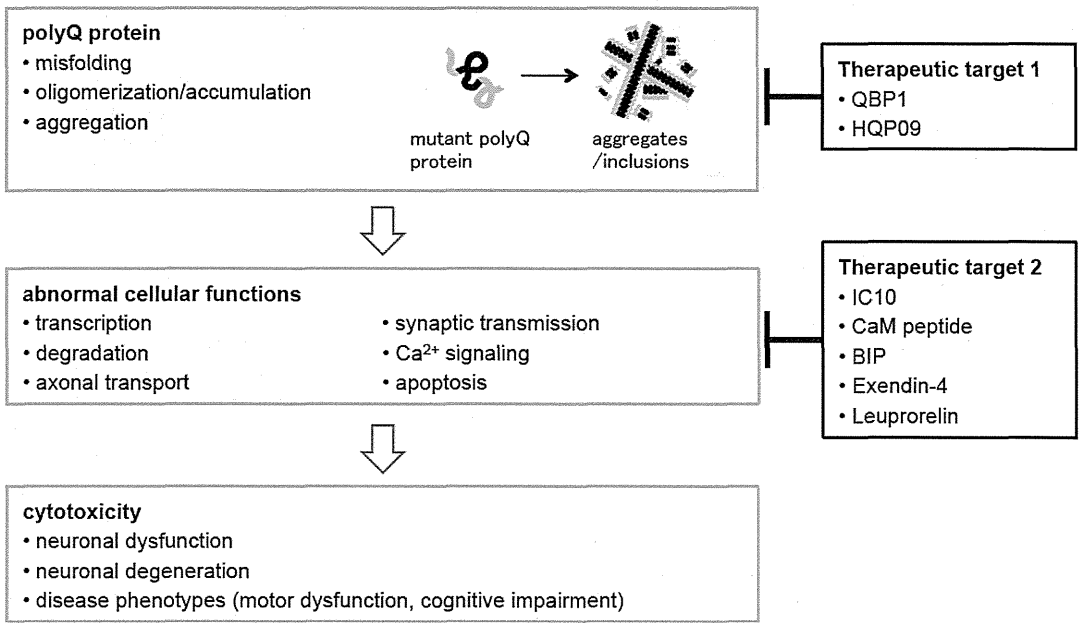

Fig. (1). Proposed mechanism of expanded polyQ protein toxicity and potential therapeutic targets for polyQ disease therapies.

Table 1. Selected examples of peptides potentially effective for the polyQ diseases.

Peptide	Sequence	Therapeutic Target	Effects *In Vitro*	Effects *In Vivo*	Ref
QBP1	SNWKWWPGIFD	polyQ aggregation	Aggregation ↓ Inclusion bodies ↓ Cytotoxicity ↓	Inclusion bodies ↓ Life span ↑ Body weight ↑	[23, 39, 54-60, 62, 63]
HQP09	Npip-Nmba-P-Nmea-Nall-Nlys-Nser[a]	polyQ aggregation	Aggregation ↓ Cytotoxicity ↓	Stabilize Ca^{2+} signaling ↓ Apoptosis ↓ Inclusion bodies	[64]
IC10	A cytosolic C-terminal tail of $InsP_3R1$ (122 amino acids)	Aberrant interaction between Htt and $InsP_3R1$	Stabilize Ca^{2+} signaling ↓	Motor function ↑ Neuronal loss ↓	[68]
CaM peptide	MKDTDSEEEIREAFRVFDKDGNGY-ISAAELRHVMTNLGEKLTDEEV (A fragment of CaM, residues 76-121)	Abberant interaction between Htt and CaM	Cytotoxicity ↓	Body weight ↑ Motor function ↑ Inclusion bodies ↓	[69-71]
BIP	VPMLK/VPTLK	Bax-induced apoptosis	Apoptosis ↓	-	[75,76]
Exendin-4	HGEGTFTSDLSKQMEEEAVRLFIEWL KNGGPSSGAPPPS	Abnormal energy metabolism	-	Motor function ↑ Life span ↑ Inclusion bodies ↓	[85]
Leuprorelin	Pyr-HWSY*LL*RP-NHEt[b,c]	Nuclear accumulation of mutant AR	-	Motor function ↑ Life span ↑ Inclusion bodies ↓	[90-92]

[a]N-substituted glycines. Npip, piperonyl; Nmba, methylbenzyl; Nmea, methoxyethyl; Nall, allyl; Nlys, aminobutyl; Nser, hydroxyethyl. [b]Pyr, pyroglutamyl. [c]*d*-amino acids in *Italics*.

QBP1

We previously took a combinatorial screening approach to search for short peptides that selectively and specifically bind to an expanded polyQ stretch, but not to a normal length polyQ stretch, using the phage display technique. Multiple rounds of screening resulted in six peptides that preferentially bind to the abnormally expanded polyQ stretch [39]. One of these peptides, QBP1 (polyQ binding peptide 1), had a particularly high affinity for the abnormal polyQ stretch with a dissociation constant (K_d) of 5.7 μM [54], and also had a suppressive effect on polyQ aggregation *in vitro* [39]. Studies focusing on its structure-activity relationship revealed that the tryptophan-rich sequence is necessary for the inhibitory activity of QBP1 [55-57]. Expression of QBP1 effectively suppressed inclusion body formation and cytotoxicity of expanded polyQ proteins in cell culture [23,39,58,59] and *Drosophila* models of the polyQ diseases [60]. Since QBP1 is poorly membrane permeable, we employed protein transduction domains (PTDs) [61] to improve the bioavailability of QBP1 by its efficient intracellular delivery. We found that the delivery efficiency of QBP1 was dramatically improved by conjugation with a PTD, leading to successful suppression of polyQ inclusions as well as polyQ-induced premature death in *Drosophila* by its oral administration [62]. The therapeutic potential of PTD-QBP1 was further investigated using a mouse model of HD. However, the therapeutic effect of PTD-QBP1 was limited to neither inhibition of body weight loss with any improvement in the other disease phenotypes nor inhibition of aggregate formation in the brains, probably due to low efficiency of PTD-QBP1 delivery to the mouse brain by intraperitoneal injections [63].

HQP09

Chen *et al.* also performed combinatorial screening to search for potential inhibitors of polyQ aggregation [64]. In contrast to our approach using peptide-based phage display libraries, they used a combinatorial library consisting of peptoids as scaffolds. Peptoids, which are oligomers of N-substituted glycines, have an advantage in developing therapeutic molecules since they are considered to be superior in stability to protease degradation, cell permeability, and structural diversity [65, 66]. They prepared a peptoid library containing 60,000 unique compounds, and screened for molecules that specifically bind to the Htt fragment with an expanded polyQ stretch. The peptoid HQP09, which was isolated from this screening process, was found to bind with high specificity to the expanded polyQ forms of Htt and ataxin-3, which is the causative protein of SCA3, and to effectively suppress polyQ aggregation *in vitro*. Interestingly, although HQP09 and QBP1 had comparable binding affinity to mutant Htt proteins, HQP09 did not show any competition with QBP1 in binding, possibly indicating that these two inhibitors recognize the abnormally expanded polyQ stretches in a different manner. The authors also tested the therapeutic activity of this peptoid, and confirmed that HQP09 reduced cytotoxicity in primary cultured neurons and decreased polyQ inclusion bodies in a mouse model of HD upon its intracerebroventricular injection. Importantly, they successfully identified the pharmacophore of HQP09 based on a structure-activity relationship study, and developed the minimal derivative peptoid HQP09-9 (4-mer, MW = 585) without significant loss of activity. Although HQP09-9 failed to exert therapeutic effects on a mouse model upon its subcu-

taneous injection probably due to poor blood-brain barrier permeability, this could be a promising lead compound for the development of drugs against a broad spectrum of the polyQ diseases.

PEPTIDE-BASED MODULATORS OF POLYGLUTAMINE TOXICITY

Another therapeutic approach is to target the various cellular dysfunctions occurring in the cascade of polyQ pathogenesis. Although the mechanisms as to how these abnormalities contribute to eventual neurodegeneration in various regions of the brain are not known, normalizing such dysfunctions has been shown to effectively reduce the toxicity of the expanded polyQ proteins and improve disease phenotypes in polyQ disease animal models.

IC10 peptide

Since aberrant interactions between mutant Htt and various proteins often cause abnormalities in downstream cellular functions [50], disruption of such interactions could be a promising therapeutic approach. Bezprozvanny and coworkers found that the polyQ expanded Htt protein specifically binds to type 1 inositol 1,4,5-triphosphate receptor ($InsP_3R1$) and facilitates its activity, indicating that abnormal neuronal Ca^{2+} signaling may play an important role in HD pathogenesis [48, 67]. Since mutant Htt specifically binds to the C-terminal cytosolic region of $InsP_3R1$ (IC10 fragment), they hypothesized that introduction of the IC10 peptide into neurons would normalize Ca^{2+} signaling and eventual neurodegeneration by interfering with the abnormal interaction between mutant Htt and $InsP_3R1$[48]. They indeed found that viral vector-mediated expression of the IC10 peptide effectively stabilized neuronal Ca^{2+} signaling, improved motor dysfunctions and reduced neuronal loss in a mouse model of HD [68].

CaM-peptide

Mutant Htt also associates with calmodulin (CaM) with a higher affinity than wild-type Htt, and this interaction facilitates a wide range of downstream cellular functions. Muma and coworkers prepared several deletion mutants of CaM and found that a fragment corresponding to 76-121 amino acids of CaM (CaM-peptide) is responsible for binding with mutant Htt [69]. They demonstrated that expression of CaM-peptide reduced cytotoxicity by disrupting the abnormal interaction between endogenous CaM and mutant Htt in cellular models [69, 70] and improved disease phenotypes including body weight loss and motor dysfunctions in a mouse model of HD [71]. The studies on both IC10 and CaM peptides strongly indicate that abnormal interactions of the expanded polyQ proteins is critical for polyQ disease pathogenesis, and that molecules targeting these abnormal interactions may be promising lead compounds for polyQ disease treatment.

BIP

It has been reported that expanded polyQ proteins directly induce apoptosis. Mutant Htt with expanded polyQ stretch was shown to activate p53 and increase the expression level of Bax, a proapoptotic member of the Bcl-2 family of proteins that play a key role in programmed cell death in neurons [72]. Similarly, activation of Bax and subsequent cell death has also been shown in cells expressing polyQ-expanded ataxin-3 and ataxin-7, causative proteins of SCA3 and SCA7, respectively [73, 74]. Matsuyama, Yokota and coworkers found that the proapoptotic activity of Bax is normally suppressed by Ku70, a cytoprotective protein that interacts with Bax and prevents its mitochondrial translocation, while in SCA3, mutant ataxin-3 abnormally stimulates the acetylation of Ku70, which results in dissociation of Bax from Ku70 and promotes the subsequent activation of apoptosis [75]. Importantly, expression of Ku70 effectively blocked mutant ataxin-3-induced cell death, which strongly indicates that approaches targeting the activation process of Bax could be effective for suppression of the eventual apoptosis induced by expanded polyQ proteins [75]. To develop peptide-based suppressors of Bax-induced apoptosis, they identified the Bax-binding domain of Ku70 and designed a penta-peptide, Bax-inhibiting peptide (BIP) derived from this domain [76]. BIP is particularly promising since this is cell-permeable and effectively suppresses the mitochondrial translocation of Bax and subsequent apoptotic cell death [75].

Exendin-4

Although the polyQ diseases are considered primarily as neurological disorders, patients also exhibit peripheral symptoms. In HD, it is known that patients suffer from various metabolic abnormalities including progressive weight loss, appetite dysfunction and poor glycemic control [77-80]. Similarly, mouse models of HD also exhibit these symptoms, together with impaired glucose metabolism in both brain and periphery and elevated blood glucose levels [81, 82]. This is probably due to the significant toxicity caused by high levels of mutant Htt in peripheral tissues including the pancreatic islet cells, leading to decrease in β-cell mass and impaired insulin release capacity [81, 82]. Since molecules that improve abnormal energy metabolism such as creatine have been shown to work as a neuroprotective agent and to delay the onset of motor dysfunction in a mouse model of HD [83], therapeutic approaches targeting this diabetic-like condition may be promising. Exendin-4 (Ex-4) is an agonist for glucagon-like peptide-1 receptor, and is used as a peptide drug for diabetes to improve glucose regulation [84]. Martin *et al.* tested the effects of Ex-4 on a mouse model of HD, and found that daily administration of Ex-4 by subcutaneous injection improved motor dysfunction and extended the life span of HD mice [85]. They also found that Ex-4 injection significantly promoted pancreatic β-cell growth and reduced Htt aggregates in the pancreas as well as in the brain cortex [85]. This study strongly indicates that therapeutic approaches targeting not only the central pathophysiologies but also the peripheral symptoms could be an effective strategy for treatment of the polyQ diseases.

Leuprorelin

SBMA is an adult-onset motor neuron disease, which is caused by the expansion of a polyQ stretch in the androgen receptor (AR) [86]. Although the specific pathogenic mechanisms of SBMA still remain unclear, the nuclear accumulation of abnormal AR proteins is thought to be respon-

sible for neuronal toxicity. Since testosterone binds to AR as a ligand and induces its nuclear translocation, reduction of the testosterone level would lead to a decrease in the eventual nuclear accumulation of mutant AR and to lower cytotoxicity [87, 88]. This idea is actually supported by the experimental fact that surgical castration significantly improved motor dysfunctions of a mouse model of SBMA [87, 89]. Katsuno *et al.* tested the effects of leuprorelin, a lutenizing hormone-releasing hormone (LHRH) peptide agonist that reduces testosterone release from the testis, and found that subcutaneous injection of leuprorelin reduced the nuclear accumulation of mutant AR in muscle and spinal cord, and improved the motor dysfunctions and extended the life span of a SBMA mouse model [90]. Furthermore, they conducted a series of clinical trials of leuprorelin including a randomized, placebo-controlled trial in a large cohort of 204 SBMA patients from 14 hospitals in Japan [91, 92]. Although clinical outcomes of leuprorelin administration for 48 weeks were limited to suppression of nuclear AR accumulation and decreased serum levels of testosterone with no significant improvement of motor functions, there is a possibility that leuprorelin could be effective in long-term trials in early-phase SBMA patients.

FUTURE DIRECTIONS

In this review, we introduced selected studies focusing on the development of peptide-based therapies for treatment of the polyQ diseases. Among them, the therapeutic approach focusing on aggregate formation of the expanded polyQ stretch, which targets the most upstream change occurring in the polyQ diseases, is considered to be most attractive because potential inhibitors are expected to suppress a large number of downstream functional abnormalities in a broad range of the polyQ diseases. However, efficient delivery into brains is always problematic in developing peptide-based drugs [93], as aggregation inhibitors developed by us [63] and by Chen *et al.* [64] both failed to demonstrate therapeutic effects on mouse models via their subcutaneous or intraperitoneal administration. Since both QBP1 and HQP09 have been shown to possess high potential to specifically and selectively suppress mutant polyQ-induced cytotoxicity, it is highly likely that they would be promising leads for development of polyQ disease drugs if given the ability to efficiently translocate across the blood-brain barrier (BBB). Therefore, it is quite clear that one of the future directions that we should progress toward is to re-design these potential peptide inhibitors into BBB-permeable molecules. Elucidating the structural basis as to how QBP1 and HQP09 inhibit aggregate formation of the expanded polyQ stretch would be helpful towards designing their small chemical analogues with high BBB permeability without loss of its inhibitory activity. Another direction is to develop effective delivery systems using carrier molecules which would efficiently deliver cargoes to the brain. Potential carriers include cell-penetrating peptides (CPPs, protein transduction domains/PTDs) [94-96], viral vectors [97, 98] and liposomes [99, 100], which may enable these peptide inhibitors to translocate through the BBB and to perform their therapeutic activities in specific regions of the brain. We hope that in the near future therapeutic approaches that are widely effective against the polyQ diseases are developed, and bring hope to many patients suffering from the currently untreatable polyQ diseases.

CONFLICT OF INTEREST

The authors confirm that this article content has no conflicts of interest.

ACKNOWLEDGEMENTS

We thank James R. Burke, Warren J. Strittmatter, Shinya Oishi and Nobutaka Fujii for their helpful discussions. The authors' work on the polyglutamine diseases is supported in part by Grants-in-Aid for Scientific Research on Priority Areas (Advanced Brain Science Project, and Research on Pathomechanisms of Brain Disorders to Y.N.) from the Ministry of Education, Culture, Sports, Science, and Technology, Japan; by Grants-in-Aid for Scientific Research (B) (to Y.N.) and Challenging Exploratory Research (to Y.N.) from the Japan Society for the Promotion of Science (JSPS), Japan; by a Grant-in-Aid for the Research Committee for Ataxic Diseases (to Y.N.) from the Ministry of Health, Labor and Welfare, Japan; and by a grant from Core Research for Evolutional Science and Technology (CREST) of the Japan Science and Technology Agency (to Y.N.). T.T. is grateful for the JSPS research fellowship.

ABBREVIATIONS

AR	=	Androgen receptor
Bax	=	Bcl-2 associated X protein
BBB	=	Blood-brain barrier
Bcl2	=	B-cell lymphoma 2
BIP	=	Bax-inhibiting peptide
CaM	=	Calmodulin
Ex-4	=	Exendin-4
HD	=	Huntington's disease
Htt	=	Huntingtin
$InsP_3R1$	=	Type 1 inositol 1,4,5-triphosphate receptor
K_d	=	Dissociation constant
LHRH	=	Lutenizing hormone-releasing hormone
MW	=	Molecular weight
PolyQ	=	Polyglutamine
PTD	=	Protein transduction domain
QBP1	=	PolyQ binding peptide 1
SBMA	=	Spinal and bulbar muscular atrophy
SCA	=	Spinocerebeller ataxia

REFERENCES

[1] Gusella, J.F.; MacDonald, M.E. Molecular genetics: unmasking polyglutamine triggers in neurodegenerative disease. *Nat. Rev. Neurosci.,* **2000**, *1*, 109-115.

[2] Orr, H.T.; Zoghbi, H.Y. Trinucleotide repeat disorders. *Annu. Rev. Neurosci.,* **2007**, *30*, 575-621.

[3] Nagai, Y.; Popiel, H.A. Conformational changes and aggregation of expanded polyglutamine proteins as therapeutic targets of the

polyglutamine diseases: exposed beta-sheet hypothesis. *Curr. Pharm. Des.,* **2008**, *14*, 3267-3279.

[4] The Huntington's Disease Collaborative Research Group. A novel gene containing a trinucleotide repeat that is expanded and unstable on Huntington's disease chromosomes. *Cell,* **1993**, *72*, 971-983.

[5] Doyu, M.; Sobue, G.; Mukai, E.; Kachi, T.; Yasuda, T.; Mitsuma, T.; Takahashi, A. Severity of X-linked recessive bulbospinal neuronopathy correlates with size of the tandem CAG repeat in androgen receptor gene. *Ann. Neurol.,* **1992**, *32*, 707-710.

[6] Igarashi, S.; Tanno, Y.; Onodera, O.; Yamazaki, M.; Sato, S.; Ishikawa, A.; Miyatani, N.; Nagashima, M.; Ishikawa, Y.; Sahashi, K.; *et al.* Strong correlation between the number of CAG repeats in androgen receptor genes and the clinical onset of features of spinal and bulbar muscular atrophy. *Neurology,* **1992**, *42*, 2300-2302.

[7] Mangiarini, L.; Sathasivam, K.; Seller, M.; Cozens, B.; Harper, A.; Hetherington, C.; Lawton, M.; Trottier, Y.; Lehrach, H.; Davies, S. W.; Bates, G. P. Exon 1 of the HD gene with an expanded CAG repeat is sufficient to cause a progressive neurological phenotype in transgenic mice. *Cell,* **1996**, *87*, 493-506.

[8] Ikeda, H.; Yamaguchi, M.; Sugai, S.; Aze, Y.; Narumiya, S.; Kakizuka, A. Expanded polyglutamine in the Machado-Joseph disease protein induces cell death *in vitro* and *in vivo*. *Nat. Genet.,* **1996**, *13*, 196-202.

[9] Burright, E.N.; Clark, H.B.; Servadio, A.; Matilla, T.; Feddersen, R.M.; Yunis, W.S.; Duvick, L.A.; Zoghbi, H.Y.; Orr, H.T. SCA1 transgenic mice: a model for neurodegeneration caused by an expanded CAG trinucleotide repeat. *Cell,* **1995**, *82*, 937-948.

[10] Warrick, J.M.; Paulson, H.L.; Gray-Board, G.L.; Bui, Q.T.; Fischbeck, K.H.; Pittman, R.N.; Bonini, N.M. Expanded polyglutamine protein forms nuclear inclusions and causes neural degeneration in Drosophila. *Cell,* **1998**, *93*, 939-949.

[11] Faber, P.W.; Alter, J.R.; MacDonald, M.E.; Hart, A.C. Polyglutamine-mediated dysfunction and apoptotic death of a Caenorhabditis elegans sensory neuron. *Proc. Natl. Acad. Sci. USA,* **1999**, *96*, 179-184.

[12] Ross, C.A. Polyglutamine pathogenesis: emergence of unifying mechanisms for Huntington's disease and related disorders. *Neuron,* **2002**, *35*, 819-822.

[13] Shao, J.; Diamond, M.I. Polyglutamine diseases: emerging concepts in pathogenesis and therapy. *Hum. Mol. Genet.,* **2007**, *16 Spec No. 2*, R115-R123.

[14] Scherzinger, E.; Lurz, R.; Turmaine, M.; Mangiarini, L.; Hollenbach, B.; Hasenbank, R.; Bates, G. P.; Davies, S.W.; Lehrach, H.; Wanker, E.E. Huntingtin-encoded polyglutamine expansions form amyloid-like protein aggregates *in vitro* and *in vivo*. *Cell,* **1997**, *90*, 549-558.

[15] Scherzinger, E.; Sittler, A.; Schweiger, K.; Heiser, V.; Lurz, R.; Hasenbank, R.; Bates, G.P.; Lehrach, H.; Wanker, E.E. Self-assembly of polyglutamine-containing huntingtin fragments into amyloid-like fibrils: implications for Huntington's disease pathology. *Proc. Natl. Acad. Sci. USA,* **1999**, *96*, 4604-4609.

[16] Chen, S.; Berthelier, V.; Yang, W.; Wetzel, R. Polyglutamine aggregation behavior *in vitro* supports a recruitment mechanism of cytotoxicity. *J. Mol. Biol.,* **2001**, *311*, 173-182.

[17] Yang, W.; Dunlap, J.R.; Andrews, R.B.; Wetzel, R. Aggregated polyglutamine peptides delivered to nuclei are toxic to mammalian cells. *Hum. Mol. Genet.,* **2002**, *11*, 2905-2917.

[18] Wetzel, R. Physical chemistry of polyglutamine: intriguing tales of a monotonous sequence. *J. Mol. Biol.,* **2012**, *421*, 466-490.

[19] Kuemmerle, S.; Gutekunst, C.A.; Klein, A.M.; Li, X.J.; Li, S.H.; Beal, M.F.; Hersch, S.M.; Ferrante, R.J. Huntington aggregates may not predict neuronal death in Huntington's disease. *Ann. Neurol.,* **1999**, *46*, 842-849.

[20] Klement, I.A.; Skinner, P.J.; Kaytor, M.D.; Yi, H.; Hersch, S.M.; Clark, H.B.; Zoghbi, H.Y.; Orr, H.T. Ataxin-1 nuclear localization and aggregation: role in polyglutamine-induced disease in SCA1 transgenic mice. *Cell,* **1998**, *95*, 41-53.

[21] Saudou, F.; Finkbeiner, S.; Devys, D.; Greenberg, M.E. Huntingtin acts in the nucleus to induce apoptosis but death does not correlate with the formation of intranuclear inclusions. *Cell,* **1998**, *95*, 55-66.

[22] Arrasate, M.; Mitra, S.; Schweitzer, E.S.; Segal, M.R.; Finkbeiner, S. Inclusion body formation reduces levels of mutant huntingtin and the risk of neuronal death. *Nature,* **2004**, *431*, 805-810.

[23] Nagai, Y.; Inui, T.; Popiel, H.A.; Fujikake, N.; Hasegawa, K.; Urade, Y.; Goto, Y.; Naiki, H.; Toda, T. A toxic monomeric conformer of the polyglutamine protein. *Nat. Struct. Mol. Biol.,* **2007**, *14*, 332-340.

[24] Cummings, C.J.; Mancini, M.A.; Antalffy, B.; DeFranco, D.B.; Orr, H.T.; Zoghbi, H.Y. Chaperone suppression of aggregation and altered subcellular proteasome localization imply protein misfolding in SCA1. *Nat. Genet.,* **1998**, *19*, 148-154.

[25] Warrick, J.M.; Chan, H.Y.; Gray-Board, G.L.; Chai, Y.; Paulson, H.L.; Bonini, N.M. Suppression of polyglutamine-mediated neurodegeneration in Drosophila by the molecular chaperone HSP70. *Nat. Genet.,* **1999**, *23*, 425-428.

[26] Sittler, A.; Lurz, R.; Lueder, G.; Priller, J.; Lehrach, H.; Hayer-Hartl, M.K.; Hartl, F.U.; Wanker, E.E. Geldanamycin activates a heat shock response and inhibits huntingtin aggregation in a cell culture model of Huntington's disease. *Hum. Mol. Genet.,* **2001**, *10*, 1307-1315.

[27] Katsuno, M.; Sang, C.; Adachi, H.; Minamiyama, M.; Waza, M.; Tanaka, F.; Doyu, M.; Sobue, G. Pharmacological induction of heat-shock proteins alleviates polyglutamine-mediated motor neuron disease. *Proc. Natl. Acad. Sci. USA,* **2005**, *102*, 16801-16806.

[28] Fujikake, N.; Nagai, Y.; Popiel, H.A.; Okamoto, Y.; Yamaguchi, M.; Toda, T. Heat shock transcription factor 1-activating compounds suppress polyglutamine-induced neurodegeneration through induction of multiple molecular chaperones. *J. Biol. Chem.,* **2008**, *283*, 26188-26197.

[29] Lecerf, J.M.; Shirley, T.L.; Zhu, Q.; Kazantsev, A.; Amersdorfer, P.; Housman, D.E.; Messer, A.; Huston, J.S. Human single-chain Fv intrabodies counteract *in situ* huntingtin aggregation in cellular models of Huntington's disease. *Proc. Natl. Acad. Sci. USA,* **2001**, *98*, 4764-4769.

[30] Colby, D.W.; Chu, Y.; Cassady, J.P.; Duennwald, M.; Zazulak, H.; Webster, J.M.; Messer, A.; Lindquist, S.; Ingram, V.M.; Wittrup, K.D. Potent inhibition of huntingtin aggregation and cytotoxicity by a disulfide bond-free single-domain intracellular antibody. *Proc. Natl. Acad. Sci. USA,* **2004**, *101*, 17616-17621.

[31] Wolfgang, W.J.; Miller, T.W.; Webster, J.M.; Huston, J.S.; Thompson, L.M.; Marsh, J.L.; Messer, A. *Proc. Natl. Acad. Sci. USA,* **2005**, *102*, 11563-11568.

[32] Nagai, Y.; Fujikake, N.; Popiel, H.A.; Wada, K. Induction of molecular chaperones as a therapeutic strategy for the polyglutamine diseases. *Curr. Pharm. Biotechnol.,* **2010**, *11*, 188-197.

[33] Butler, D.C.; McLear, J.A.; Messer, A. Engineered antibody therapies to counteract mutant huntingtin and related toxic intracellular proteins. *Prog. Neurobiol.,* **2012**, *97*, 190-204.

[34] Heiser, V.; Scherzinger, E.; Boeddrich, A.; Nordhoff, E.; Lurz, R.; Schugardt, N.; Lehrach, H.; Wanker, E.E. Inhibition of huntingtin fibrillogenesis by specific antibodies and small molecules: implications for Huntington's disease therapy. *Proc. Natl. Acad. Sci. USA,* **2000**, *97*, 6739-6744.

[35] Heiser, V.; Engemann, S.; Brocker, W.; Dunkel, I.; Boeddrich, A.; Waelter, S.; Nordhoff, E.; Lurz, R.; Schugardt, N.; Rautenberg, S.; Herhaus, C.; Barnickel, G.; Bottcher, H.; Lehrach, H.; Wanker, E.E. Identification of benzothiazoles as potential polyglutamine aggregation inhibitors of Huntington's disease by using an automated filter retardation assay. *Proc. Natl. Acad. Sci. USA,* **2002**, *99 Suppl 4*, 16400-16406.

[36] Tanaka, M.; Machida, Y.; Niu, S.; Ikeda, T.; Jana, N.R.; Doi, H.; Kurosawa, M.; Nekooki, M.; Nukina, N. Trehalose alleviates polyglutamine-mediated pathology in a mouse model of Huntington disease. *Nat. Med.,* **2004**, *10*, 148-154.

[37] Wang, J.; Gines, S.; MacDonald, M.E.; Gusella, J.F. Reversal of a full-length mutant huntingtin neuronal cell phenotype by chemical inhibitors of polyglutamine-mediated aggregation. *BMC. Neurosci.,* **2005**, *6*, 1.

[38] Ehrnhoefer, D.E.; Duennwald, M.; Markovic, P.; Wacker, J.L.; Engemann, S.; Roark, M.; Legleiter, J.; Marsh, J.L.; Thompson, L.M.; Lindquist, S.; Muchowski, P.J.; Wanker, E.E. Green tea (-)-epigallocatechin-gallate modulates early events in huntingtin misfolding and reduces toxicity in Huntington's disease models. *Hum. Mol. Genet.,* **2006**, *15*, 2743-2751.

[39] Nagai, Y.; Tucker, T.; Ren, H.; Kenan, D.J.; Henderson, B.S.; Keene, J.D.; Strittmatter, W.J.; Burke, J.R. Inhibition of polyglutamine protein aggregation and cell death by novel peptides identified by phage display screening. *J. Biol. Chem.,* **2000**, *275*, 10437-10442.

[40] Kazantsev, A.; Walker, H.A.; Slepko, N.; Bear, J.E.; Preisinger, E.; Steffan, J.S.; Zhu, Y.Z.; Gertler, F.B.; Housman, D.E.; Marsh, J.L.; Thompson, L.M. A bivalent Huntingtin binding peptide suppresses polyglutamine aggregation and pathogenesis in Drosophila. *Nat. Genet.,* **2002**, *30*, 367-376.

[41] Popiel, H.A.; Nagai, Y.; Onodera, O.; Inui, T.; Fujikake, N.; Urade, Y.; Strittmatter, W.J.; Burke, J.R.; Ichikawa, A.; Toda, T. Disruption of the toxic conformation of the expanded polyglutamine stretch leads to suppression of aggregate formation and cytotoxicity. *Biochem. Biophys. Res. Commun.,* **2004**, *317*, 1200-1206.

[42] Bauer, P.O.; Goswami, A.; Wong, H.K.; Okuno, M.; Kurosawa, M.; Yamada, M.; Miyazaki, H.; Matsumoto, G.; Kino, Y.; Nagai, Y.; Nukina, N. Harnessing chaperone-mediated autophagy for the selective degradation of mutant huntingtin protein. *Nat. Biotechnol.,* **2010**, *28*, 256-263.

[43] Shoji-Kawata, S.; Sumpter, R.; Leveno, M.; Campbell, G.R.; Zou, Z.; Kinch, L.; Wilkins, A.D.; Sun, Q.; Pallauf, K.; MacDuff, D.; Huerta, C.; Virgin, H.W.; Helms, J.B.; Eerland, R.; Tooze, S.A.; Xavier, R.; Lenschow, D.J.; Yamamoto, A.; King, D.; Lichtarge, O.; Grishin, N.V.; Spector, S.A.; Kaloyanova, D.V.; Levine, B. Identification of a candidate therapeutic autophagy-inducing peptide. *Nature,* **2013**, *494*, 201-206.

[44] Steffan, J.S.; Kazantsev, A.; Spasic-Boskovic, O.; Greenwald, M.; Zhu, Y.Z.; Gohler, H.; Wanker, E.E.; Bates, G.P.; Housman, D.E.; Thompson, L.M. The Huntington's disease protein interacts with p53 and CREB-binding protein and represses transcription. *Proc. Natl. Acad. Sci. USA,* **2000**, *97*, 6763-6768.

[45] Bence, N.F.; Sampat, R.M.; Kopito, R.R. Impairment of the ubiquitin-proteasome system by protein aggregation. *Science,* **2001**, *292*, 1552-1555.

[46] Romero, E.; Cha, G.H.; Verstreken, P.; Ly, C.V.; Hughes, R.E.; Bellen, H.J.; Botas, J. Suppression of neurodegeneration and increased neurotransmission caused by expanded full-length huntingtin accumulating in the cytoplasm. *Neuron,* **2008**, *57*, 27-40.

[47] Gunawardena, S.; Her, L.S.; Brusch, R.G.; Laymon, R.A.; Niesman, I.R.; Gordesky-Gold, B.; Sintasath, L.; Bonini, N.M.; Goldstein, L.S. Disruption of axonal transport by loss of huntingtin or expression of pathogenic polyQ proteins in Drosophila. *Neuron,* **2003**, *40*, 25-40.

[48] Tang, T.S.; Tu, H.; Chan, E.Y.; Maximov, A.; Wang, Z.; Wellington, C.L.; Hayden, M.R.; Bezprozvanny, I. Huntingtin and huntingtin-associated protein 1 influence neuronal calcium signaling mediated by inositol-(1,4,5) triphosphate receptor type 1. *Neuron,* **2003**, *39*, 227-239.

[49] Tobin, A.J.; Signer, E.R. Huntington's disease: the challenge for cell biologists. *Trends Cell Biol.,* **2000**, *10*, 531-536.

[50] Harjes, P.; Wanker, E.E. The hunt for huntingtin function: interaction partners tell many different stories. *Trends Biochem. Sci.,* **2003**, *28*, 425-433.

[51] Trottier, Y.; Lutz, Y.; Stevanin, G.; Imbert, G.; Devys, D.; Cancel, G.; Saudou, F.; Weber, C.; David, G.; Tora, L.; Agid, Y.; Brice, A.; Mandel, J. Polyglutamine expansion as a pathological epitope in Huntington's disease and four dominant cerebellar ataxias. *Nature,* **1995**, *378*, 403-406.

[52] Bennett, M.J.; Huey-Tubman, K.E.; Herr, A.B.; West, A.P., Jr.; Ross, S.A.; Bjorkman, P.J. A linear lattice model for polyglutamine in CAG-expansion diseases. *Proc. Natl. Acad. Sci. USA,* **2002**, *99*, 11634-11639.

[53] Miller, J.; Arrasate, M.; Brooks, E.; Libeu, C.P.; Legleiter, J.; Hatters, D.; Curtis, J.; Cheung, K.; Krishnan, P.; Mitra, S.; Widjaja, K.; Shaby, B.A.; Lotz, G.P.; Newhouse, Y.; Mitchell, E.J.; Osmand, A.; Gray, M.; Thulasiramin, V.; Saudou, F.; Segal, M.; Yang, X.W.; Masliah, E.; Thompson, L.M.; Muchowski, P.J.; Weisgraber, K.H.; Finkbeiner, S. Identifying polyglutamine protein species in situ that best predict neurodegeneration. *Nat. Chem. Biol.,* **2011**, *7*, 925-934.

[54] Okamoto, Y.; Nagai, Y.; Fujikake, N.; Popiel, H.A.; Yoshioka, T.; Toda, T.; Inui, T. Surface plasmon resonance characterization of specific binding of polyglutamine aggregation inhibitors to the expanded polyglutamine stretch. *Biochem. Biophys. Res. Commun.,* **2009**, *378*, 634-639.

[55] Ren, H.; Nagai, Y.; Tucker, T.; Strittmatter, W.J.; Burke, J.R. Amino acid sequence requirements of peptides that inhibit polyglutamine-protein aggregation and cell death. *Biochem. Biophys. Res. Commun.,* **2001**, *288*, 703-710.

[56] Tomita, K.; Popiel, H.A.; Nagai, Y.; Toda, T.; Yoshimitsu, Y.; Ohno, H.; Oishi, S.; Fujii, N. Structure-activity relationship study on polyglutamine binding peptide QBP1. *Bioorg. Med. Chem.,* **2009**, *17*, 1259-1263.

[57] Hamuro, L.; Zhang, G.; Tucker, T.J.; Self, C.; Strittmatter, W.J.; Burke, J.R. Optimization of a polyglutamine aggregation inhibitor peptide (QBP1) using a thioflavin T fluorescence assay. *Assay Drug Dev. Technol.,* **2007**, *5*, 629-636.

[58] Takahashi, Y.; Okamoto, Y.; Popiel, H.A.; Fujikake, N.; Toda, T.; Kinjo, M.; Nagai, Y. Detection of polyglutamine protein oligomers in cells by fluorescence correlation spectroscopy. *J. Biol. Chem.,* **2007**, *282*, 24039-24048.

[59] Takahashi, T.; Kikuchi, S.; Katada, S.; Nagai, Y.; Nishizawa, M.; Onodera, O. Soluble polyglutamine oligomers formed prior to inclusion body formation are cytotoxic. *Hum. Mol. Genet.,* **2008**, *17*, 345-356.

[60] Nagai, Y.; Fujikake, N.; Ohno, K.; Higashiyama, H.; Popiel, H.A.; Rahadian, J.; Yamaguchi, M.; Strittmatter, W.J.; Burke, J.R.; Toda, T. Prevention of polyglutamine oligomerization and neurodegeneration by the peptide inhibitor QBP1 in Drosophila. *Hum. Mol. Genet.,* **2003**, *12*, 1253-1259.

[61] Futaki, S.; Hirose, H.; Nakase, I. Arginine-rich peptides: methods of translocation through biological membranes. *Curr. Pharm. Des.,* **2012**, *19*, 2863-2868.

[62] Popiel, H.A.; Nagai, Y.; Fujikake, N.; Toda, T. Protein transduction domain-mediated delivery of QBP1 suppresses polyglutamine-induced neurodegeneration in vivo. *Mol. Ther.,* **2007**, *15*, 303-309.

[63] Popiel, H.A.; Nagai, Y.; Fujikake, N.; Toda, T. Delivery of the aggregate inhibitor peptide QBP1 into the mouse brain using PTDs and its therapeutic effect on polyglutamine disease mice. *Neurosci. Lett.,* **2009**, *449*, 87-92.

[64] Chen, X.; Wu, J.; Luo, Y.; Liang, X.; Supnet, C.; Kim, M.W.; Lotz, G.P.; Yang, G.; Muchowski, P.J.; Kodadek, T.; Bezprozvanny, I. Expanded polyglutamine-binding peptoid as a novel therapeutic agent for treatment of Huntington's disease. *Chem. Biol.,* **2011**, *18*, 1113-1125.

[65] Simon, R.J.; Kania, R.S.; Zuckermann, R.N.; Huebner, V.D.; Jewell, D.A.; Banville, S.; Ng, S.; Wang, L.; Rosenberg, S.; Marlowe, C.K.; Spellmeyer, D.C.; Tan, R.; Frankel, A.D.; Santi, D.V.; Cohen, F.E.; Bartlett, P.A. Peptoids: a modular approach to drug discovery. *Proc. Natl. Acad. Sci. USA,* **1992**, *89*, 9367-9371.

[66] Zuckermann, R.N.; Kodadek, T. Peptoids as potential therapeutics. *Curr. Opin. Mol. Ther.,* **2009**, *11*, 299-307.

[67] Tang, T.S.; Tu, H.; Orban, P.C.; Chan, E.Y.; Hayden, M.R.; Bezprozvanny, I. HAP1 facilitates effects of mutant huntingtin on inositol 1,4,5-trisphosphate-induced Ca release in primary culture of striatal medium spiny neurons. *Eur. J. Neurosci.,* **2004**, *20*, 1779-1787.

[68] Tang, T.S.; Guo, C.; Wang, H.; Chen, X.; Bezprozvanny, I. Neuroprotective effects of inositol 1,4,5-trisphosphate receptor C-terminal fragment in a Huntington's disease mouse model. *J. Neurosci.,* **2009**, *29*, 1257-1266.

[69] Dudek, N.L.; Dai, Y.; Muma, N.A. Protective effects of interrupting the binding of calmodulin to mutant huntingtin. *J. Neuropathol. Exp. Neurol.,* **2008**, *67*, 355-365.

[70] Dudek, N.L.; Dai, Y.; Muma, N.A. Neuroprotective effects of calmodulin peptide 76-121aa: disruption of calmodulin binding to mutant huntingtin. *Brain Pathol.,* **2010**, *20*, 176-189.

[71] Dai, Y.; Dudek, N.L.; Li, Q.; Fowler, S.C.; Muma, N.A. Striatal expression of a calmodulin fragment improved motor function, weight loss, and neuropathology in the R6/2 mouse model of Huntington's disease. *J. Neurosci.,* **2009**, *29*, 11550-11559.

[72] Bae, B.I.; Xu, H.; Igarashi, S.; Fujimuro, M.; Agrawal, N.; Taya, Y.; Hayward, S.D.; Moran, T.H.; Montell, C.; Ross, C.A.; Snyder, S.H.; Sawa, A. p53 mediates cellular dysfunction and behavioral abnormalities in Huntington's disease. *Neuron,* **2005**, *47*, 29-41.

[73] Chou, A.H.; Yeh, T.H.; Kuo, Y.L.; Kao, Y.C.; Jou, M.J.; Hsu, C.Y.; Tsai, S.R.; Kakizuka, A.; Wang, H.L. Polyglutamine-expanded ataxin-3 activates mitochondrial apoptotic pathway by upregulating Bax and downregulating Bcl-xL. *Neurobiol. Dis.,* **2006**, *21*, 333-345.

[74] Wang, H.L.; Yeh, T.H.; Chou, A.H.; Kuo, Y.L.; Luo, L.J.; He, C.Y.; Huang, P.C.; Li, A.H. Polyglutamine-expanded ataxin-7 activates mitochondrial apoptotic pathway of cerebellar neurons by

upregulating Bax and downregulating Bcl-x(L). *Cell. Signal.,* **2006**, *18*, 541-552.

[75] Li, Y.; Yokota, T.; Gama, V.; Yoshida, T.; Gomez, J.A.; Ishikawa, K.; Sasaguri, H.; Cohen, H.Y.; Sinclair, D.A.; Mizusawa, H.; Matsuyama, S. Bax-inhibiting peptide protects cells from polyglutamine toxicity caused by Ku70 acetylation. *Cell Death Differ.,* **2007**, *14*, 2058-2067.

[76] Yoshida, T.; Tomioka, I.; Nagahara, T.; Holyst, T.; Sawada, M.; Hayes, P.; Gama, V.; Okuno, M.; Chen, Y.; Abe, Y.; Kanouchi, T.; Sasada, H.; Wang, D.; Yokota, T.; Sato, E.; Matsuyama, S. Bax-inhibiting peptide derived from mouse and rat Ku70. *Biochem. Biophys. Res. Commun.,* **2004**, *321*, 961-966.

[77] Aziz, N.A.; Swaab, D.F.; Pijl, H.; Roos, R.A. Hypothalamic dysfunction and neuroendocrine and metabolic alterations in Huntington's disease: clinical consequences and therapeutic implications. *Rev. Neurosci.,* **2007**, *18*, 223-251.

[78] Powers, W.J.; Videen, T.O.; Markham, J.; McGee-Minnich, L.; Antenor-Dorsey, J.V.; Hershey, T.; Perlmutter, J.S. Selective defect of in vivo glycolysis in early Huntington's disease striatum. *Proc. Natl. Acad. Sci. USA,* **2007**, *104*, 2945-2949.

[79] Gaba, A.M.; Zhang, K.; Marder, K.; Moskowitz, C.B.; Werner, P.; Boozer, C.N. Energy balance in early-stage Huntington disease. *Am. J. Clin. Nutr.,* **2005**, *81*, 1335-1341.

[80] Lodi, R.; Schapira, A.H.; Manners, D.; Styles, P.; Wood, N.W.; Taylor, D.J.; Warner, T.T. Abnormal in vivo skeletal muscle energy metabolism in Huntington's disease and dentatorubropallidoluysian atrophy. *Ann. Neurol.,* **2000**, *48*, 72-76.

[81] Hurlbert, M.S.; Zhou, W.; Wasmeier, C.; Kaddis, F.G.; Hutton, J.C.; Freed, C.R. Mice transgenic for an expanded CAG repeat in the Huntington's disease gene develop diabetes. *Diabetes,* **1999**, *48*, 649-651.

[82] Bjorkqvist, M.; Fex, M.; Renstrom, E.; Wierup, N.; Petersen, A.; Gil, J.; Bacos, K.; Popovic, N.; Li, J.Y.; Sundler, F.; Brundin, P.; Mulder, H. The R6/2 transgenic mouse model of Huntington's disease develops diabetes due to deficient beta-cell mass and exocytosis. *Hum. Mol. Genet.,* **2005**, *14*, 565-574.

[83] Ferrante, R.J.; Andreassen, O.A.; Jenkins, B.G.; Dedeoglu, A.; Kuemmerle, S.; Kubilus, J.K.; Kaddurah-Daouk, R.; Hersch, S.M.; Beal, M.F. Neuroprotective effects of creatine in a transgenic mouse model of Huntington's disease. *J. Neurosci.,* **2000**, *20*, 4389-4397.

[84] Greig, N.H.; Holloway, H.W.; De Ore, K.A.; Jani, D.; Wang, Y.; Zhou, J.; Garant, M. J.; Egan, J.M. Once daily injection of exendin-4 to diabetic mice achieves long-term beneficial effects on blood glucose concentrations. *Diabetologia,* **1999**, *42*, 45-50.

[85] Martin, B.; Golden, E.; Carlson, O.D.; Pistell, P.; Zhou, J.; Kim, W.; Frank, B.P.; Thomas, S.; Chadwick, W.A.; Greig, N.H.; Bates, G.P.; Sathasivam, K.; Bernier, M.; Maudsley, S.; Mattson, M.P.; Egan, J.M. Exendin-4 improves glycemic control, ameliorates brain and pancreatic pathologies, and extends survival in a mouse model of Huntington's disease. *Diabetes,* **2009**, *58*, 318-328.

[86] Katsuno, M.; Tanaka, F.; Adachi, H.; Banno, H.; Suzuki, K.; Watanabe, H.; Sobue, G. Pathogenesis and therapy of spinal and bulbar muscular atrophy (SBMA). *Prog. Neurobiol.,* **2012**, *99*, 246-256.

[87] Katsuno, M.; Adachi, H.; Kume, A.; Li, M.; Nakagomi, Y.; Niwa, H.; Sang, C.; Kobayashi, Y.; Doyu, M.; Sobue, G. Testosterone reduction prevents phenotypic expression in a transgenic mouse model of spinal and bulbar muscular atrophy. *Neuron,* **2002**, *35*, 843-854.

[88] Takeyama, K.; Ito, S.; Yamamoto, A.; Tanimoto, H.; Furutani, T.; Kanuka, H.; Miura, M.; Tabata, T.; Kato, S. Androgen-dependent neurodegeneration by polyglutamine-expanded human androgen receptor in Drosophila. *Neuron,* **2002**, *35*, 855-864.

[89] Chevalier-Larsen, E.S.; O'Brien, C.J.; Wang, H.; Jenkins, S.C.; Holder, L.; Lieberman, A.P.; Merry, D.E. Castration restores function and neurofilament alterations of aged symptomatic males in a transgenic mouse model of spinal and bulbar muscular atrophy. *J. Neurosci.,* **2004**, *24*, 4778-4786.

[90] Katsuno, M.; Adachi, H.; Doyu, M.; Minamiyama, M.; Sang, C.; Kobayashi, Y.; Inukai, A.; Sobue, G. Leuprorelin rescues polyglutamine-dependent phenotypes in a transgenic mouse model of spinal and bulbar muscular atrophy. *Nat. Med.,* **2003**, *9*, 768-773.

[91] Banno, H.; Katsuno, M.; Suzuki, K.; Takeuchi, Y.; Kawashima, M.; Suga, N.; Takamori, M.; Ito, M.; Nakamura, T.; Matsuo, K.; Yamada, S.; Oki, Y.; Adachi, H.; Minamiyama, M.; Waza, M.; Atsuta, N.; Watanabe, H.; Fujimoto, Y.; Nakashima, T.; Tanaka, F.; Doyu, M.; Sobue, G. Phase 2 trial of leuprorelin in patients with spinal and bulbar muscular atrophy. *Ann. Neurol.,* **2009**, *65*, 140-150.

[92] Katsuno, M.; Banno, H.; Suzuki, K.; Takeuchi, Y.; Kawashima, M.; Yabe, I.; Sasaki, H.; Aoki, M.; Morita, M.; Nakano, I.; Kanai, K.; Ito, S.; Ishikawa, K.; Mizusawa, H.; Yamamoto, T.; Tsuji, S.; Hasegawa, K.; Shimohata, T.; Nishizawa, M.; Miyajima, H.; Kanda, F.; Watanabe, Y.; Nakashima, K.; Tsujino, A.; Yamashita, T.; Uchino, M.; Fujimoto, Y.; Tanaka, F.; Sobue, G. Efficacy and safety of leuprorelin in patients with spinal and bulbar muscular atrophy (JASMITT study): a multicentre, randomised, double-blind, placebo-controlled trial. *Lancet Neurol.,* **2010**, *9*, 875-884.

[93] Craik, D.J.; Fairlie, D.P.; Liras, S.; Price, D. The Future of Peptide-based Drugs. *Chem. Biol. Drug Des.,* **2013**, *81*, 136-147.

[94] Asoh, S.; Ohta, S. PTD-mediated delivery of anti-cell death proteins/peptides and therapeutic enzymes. *Adv. Drug Deliv. Rev.,* **2008**, *60*, 499-516.

[95] Blumling Iii, J.P.; Silva, G.A. Targeting the brain: advances in drug delivery. *Curr. Pharm. Biotechnol.,* **2012**, *13*, 2417-2426.

[96] Malakoutikhah, M.; Teixidó, M.; Giralt, E. Shuttle-mediated drug delivery to the brain. *Angew. Chem. Int. Ed.,* **2011**, *50*, 7998-8014.

[97] Salegio, E.A.; Samaranch, L.; Kells, A.P.; Forsayeth, J.; Bankiewicz, K. Guided delivery of adeno-associated viral vectors into the primate brain. *Adv. Drug Deliv. Rev.,* **2012**, *64*, 598-604.

[98] Hester, M.E.; Foust, K.D.; Kaspar, R.W.; Kaspar, B.K. AAV as a gene transfer vector for the treatment of neurological disorders: novel treatment thoughts for ALS. *Curr. Gene Ther.,* **2009**, *9*, 428-433.

[99] Garbayo, E.; Ansorena, E.; Blanco-Prieto, M.J. Brain drug delivery systems for neurodegenerative disorders. *Curr. Pharm. Biotechnol.,* **2012**, *13*, 2388-2402.

[100] Micheli, M.R.; Bova, R.; Magini, A.; Polidoro, M.; Emiliani, C. Lipid-based nanocarriers for CNS-targeted drug delivery. *Recent Pat. CNS Drug Discov.,* **2012**, *7*, 71-86.

Received: ???????????????? **Revised:** ???????????????? **Accepted:** ????????????????

OPEN ACCESS Freely available online

PLOS ONE

Na^+/H^+ Exchangers Induce Autophagy in Neurons and Inhibit Polyglutamine-Induced Aggregate Formation

Kazuya Togashi[1☯¤], Shuji Wakatsuki[1☯], Akiko Furuno[1], Shinji Tokunaga[1], Yoshitaka Nagai[2], Toshiyuki Araki[1*]

1 Department of Peripheral Nervous System Research, National Institute of Neuroscience, National Center of Neurology and Psychiatry, Kodaira, Tokyo, Japan, **2** Department of Degenerative Neurological Diseases, National Institute of Neuroscience, National Center of Neurology and Psychiatry, Kodaira, Tokyo, Japan

Abstract

In polyglutamine diseases, an abnormally elongated polyglutamine results in protein misfolding and accumulation of intracellular aggregates. Autophagy is a major cellular degradative pathway responsible for eliminating unnecessary proteins, including polyglutamine aggregates. Basal autophagy constitutively occurs at low levels in cells for the performance of homeostatic function, but the regulatory mechanism for basal autophagy remains elusive. Here we show that the Na^+/H^+ exchanger (NHE) family of ion transporters affect autophagy in a neuron-like cell line (Neuro-2a cells). We showed that expression of NHE1 and NHE5 is correlated to polyglutamine accumulation levels in a cellular model of Huntington's disease, a fatal neurodegenerative disorder characterized by accumulation of polyglutamine-containing aggregate formation in the brain. Furthermore, we showed that loss of NHE5 results in increased polyglutamine accumulation in an animal model of Huntington's disease. Our data suggest that cellular pH regulation by NHE1 and NHE5 plays a role in regulating basal autophagy and thereby promotes autophagy-mediated degradation of proteins including polyglutamine aggregates.

Citation: Togashi K, Wakatsuki S, Furuno A, Tokunaga S, Nagai Y, et al. (2013) Na^+/H^+ Exchangers Induce Autophagy in Neurons and Inhibit Polyglutamine-Induced Aggregate Formation. PLoS ONE 8(11): e81313. doi:10.1371/journal.pone.0081313

Editor: Hirofumi Arakawa, National Cancer Center Research Institute, Japan

Received September 20, 2013; **Accepted** October 16, 2013; **Published** November 21, 2013

Funding: This study is supported by grants from the Ministry of Health, Labour, and Welfare (T.A.), and Kakenhi (19800066 and 22700407, for K.T.). The funders had no role in study design, data collection and analysis, decision to publish, or preparation of the manuscript.

Competing Interests: The authors have the following interests. Yoshitaka Nagai is a PLOS ONE Editorial Board member. This does not alter the authors' adherence to all the PLOS ONE policies on sharing data and materials.

* E-mail: taraki@ncnp.go.jp.

☯ These authors contributed equally to this work.

¤ Current address: Department of Cell Biology, Osaka Bioscience Institute, Suita, Osaka, Japan

Introduction

Accumulation and aggregation of mutant proteins is a characteristic feature of a number of neurodegenerative disorders, including Parkinson's disease and Huntington's disease (HD) [1]. In HD, for example, the disease-causing mutation in huntingtin (HTT), a protein of uncertain function causes expansion of a stretch of glutamines (polyQ) near its N terminus, and the mutant form of HTT accumulates as nuclear and cytoplasmic inclusions in an HD brain [2]. One of the major therapeutic challenges in the field of neurodegeneration has been to improve the degradation of accumulated mutant proteins.

Autophagy is a cellular protein clearance mechanism and can, in principle, clear aggregation-prone proteins [3]. In this process, double-membrane organelles, called autophagosomes, engulf cellular proteins and organelles and fuse with lysosomes to form autolysosomes, which then degrade the organelle's contents [3]. Some previous reports showed that mutated HTT expression may be associated with up-regulated autophagy, and autophagy degrades polyQ-expanded proteins [4,5].

Induction of autophagy is typically observed by nutrient deprivation in many types of cells and organs and promote protein turnover to combat against starvation [6]. The brain, on the other hand, appears to be protected against energy deprivation even when the entire body is under starvation, because nutrients (e.g., amino acids, glucose, and ketone bodies) are compensated by a constant supply from other organs. Therefore, autophagy in the brain neurons does not seem to be induced by energy deprivation, indicating that regulation of autophagy in neurons is different from that in most other cell types [7].

In this study we employed Neuro-2a cell, a neuron-like cell-line, to analyze the regulatory mechanism of autophagy. We found that the function of the Na^+/H^+ exchanger (NHE) family of ion transporters affect autophagy in Neuro-2a cells. NHEs are integral membrane proteins catalyzing the exchange of Na^+ and H^+ down their respective concentration gradients and play a role in regulating a variety of physiological processes, ranging from the fine control of intracellular pH and cell volume to systemic electrolyte, acid-base and fluid volume homeostasis [8]. Here we showed that expression of NHE1 and NHE5 is correlated to polyQ accumulation levels in cellular and animal models of HD. Together, these data suggest that cellular pH regulation by NHE1 and NHE5 play a role in regulating basal autophagy in the brain's neurons.

Materials and Methods

Animals

The technical protocols for animal experiments in this study were approved by Small Animal Welfare Committee at the National Center for Neurology and Psychiatry.

NHE5 null mutant mouse strain was obtained from Deltagen Inc. (Detailed methods and confirmation for the targeted gene deletion are provided by the company upon request.) Mice overexpressing human huntingtin residues 1–171 with 82 glutamine repeats (N171-82Q mice) [9] were obtained from the Jackson Laboratory.

Cell culture

Neuro-2a cells (ATCC) were maintained using Dulbecco's modified Eagle's medium (Invitrogen) supplemented with 10% fetal bovine serum, 25 U/ml penicillin, 25 μg/ml streptomycin (Invitrogen) and 4 mM L-glutamine (Invitrogen) in a humidifying incubator at 37 C, with 5% CO2 and 95% air, unless otherwise mentioned. Lipofectamine 2000 reagent (Invitrogen) was used for plasmid DNA transfection per manufacturer's protocol. In some experiments, cells were treated with the culture media containing 200 μM DIDS (Sigma) or 10 μM EIPA (Sigma) for 2 hr, or 10 μg/ml E64d (Peptide Institute Inc) and 10 μg/ml pepstatin A (Peptide Institute Inc) for 18 hr prior to morphological or immunoblot analysis.

Construction of expression plasmids and mutagenesis

pEGFP-C1-MAP1LC3A, pEGFP-C1-MAP1LC3B, pcDNA3-NHE1, and pcDNA3-NHE5 were constructed by amplifying coding regions of the genes by RT-PCR using total RNA extracted from mouse dorsal root ganglion neurons as a template, followed by cloning into the expression plasmids. pcDNA3-NHE1E266I and pcDNA3-NHE5E212I were generated by PCR-based mutagenesis using pcDNA3-NHE1, and pcDNA3-NHE5, respectively, as templates. For construction of dKeima-mem, EGFP region of pEGFP-C1 (Clontech) vector was replaced with dKeima-Red from pdKeima-Red-S1 (Amalgaam) and c-Ha-Ras farnesylation signal (KLNPPDESGPGCMSCKCVLS) was added to the C-terminal using a PCR-based method. NLSQ81EGFP and NESQ81EGFP plasmids were constructed by inserting nuclear localization signal sequence (PKKKRKV)or nuclear exclusion signal sequence (LALKLAGLDI) followed by human atrophin1-derived polyglutamine sequence (81 glutamine with 5 amino acid-flanking sequence derived from atrophin1 at both ends) at the multiple cloning site of pEGFP-N1 plasmid (Clontech) and a myc tag sequence at C-terminus of EGFP by a PCR-based method [10]. Expression plasmids for HttEx1-Q25-EGFP and HttEx1-Q97-EGFP were provided by Dr. A. Iwata (The University of Tokyo), and HttEx1-Q25 and HttEx1-Q97 were constructed by removing EGFP regions from them. The integrity of each clone was confirmed by sequencing.

Intracellular pH measurements

For intracellular pH estimation using dKeima-mem, fluorescence was measured in standard bath solution containing 140 mM NaCl, 5 mM KCl, 2 mM $MgCl_2$, 2 mM $CaCl_2$, 10 mM HEPES, and 10 mM glucose at pH 7.4 (adjusted with NaOH). The ratio of florescence intensities of dKeima-Red emissions at 445 nm and 586 nm was calculated for intracellular pH estimation, which was based on previous report on pH measurement using dKeima-red [11]. The high-[K+]/nigericin technique was employed to convert dKeima-Red emission intensity ratios into pH_i values [12,13]. The data shown are obtained from 961 cells in 29 independent experiments for HttEx1-Q25 expressing cells, and from 960 cells in 27 independent experiments for HttEx1-Q97 expressing cells. Differences between groups were examined for statistical significance using Welch's t-test.

For characterizing NHEs expressed in Neuro-2a cells, cells were alkalinized and acidified for 2.5 min pre-pulse technique in a solution consisting of 110 mM NaCl, 30 mM NH_4Cl, 5 mM KCl, 2 mM $CaCl_2$, 2 mM $MgCl_2$, 10 mM HEPES, 10 mM glucose at pH 7.4 (adjusted with NaOH), followed by incubation for 2.5 min in a Na^+ free solution containing 140 mM NMDG, 5 mM KCl, 2 mM $CaCl_2$, 2 mM $MgCl_2$, 10 mM HEPES, 10 mM glucose at pH 7.4 (adjusted with HCl). Recovery of intracellular pH was then observed by another 2.5 min incubation in a Na^+-containing standard bath solution. Intracellular pH change profile in a representative experiment is shown in Fig 1A. The recovery of pH_i was fitted to a single exponential function using Origin Pro 8.0 (OriginLab). "pHi recovery rate" was designated as the rate of Na^+-dependent intracellular pH (pH unit per min) at 0.05 pH_i unit increments from the point of maximum acidification. Differences between groups were examined for statistical significance using Student's t-test.

Immunofluorescence staining

NHE5 null mutant mice and their wild type littermates (9 weeks of age; 3 males for each genotype) were analyzed. Immunohistochemistry procedures were carried out as described [14]. Mouse anti-HTT a.a. 1–82 monoclonal antibody (Millipore; clone 2B4) and rabbit anti-p62/SQSTM1 polyclonal antibody (MBL) were used as primary antibodies. Alexa 488-conjugated anti-rabbit IgG, andAlexa 594-conjugated anti-mouse IgG (Molecular Probes) were used as secondary antibodies. DAPI (Sigma) was used for identification of nuclei.

Image analysis for quantification

For analysis using cultured cells, 3 images were obtained from 3 independent experiments for each condition. For aggregate quantification in brain tissues, 6 images of randomly selected fields from cerebellar cortex granular layer sections were obtained from mouse brains of indicated genotypes. Fluorescent images were captured on a laser scanning microscopy (Leica TCS SP2) using ×64 objective lens (each emage is a square, 119.047619 μm each side). Aggregate numbers were counted using PhotoshopCS4 Extended edition. Diameter of aggregate was determined by regarding that the aggregate area is circular. Differences between groups were examined for statistical significance by Student's t-test for aggregate numbers, and by Mann-Whitney's U-test for aggregate diameters.

RT-PCR analysis

For detection of mRNA expression of NHE family of molecules by RT-PCR in Neuro-2a cells, the following primer sets were used: NHE1-forward (F): CACCAGTGGAACTGGACCTT; NHE1-reverse (R): AAGGTGGTCCAGGAACTGTG; NHE2-F: CAATGACTGCCGTGAAGAGA; NHE2-R: GTCCGAGTCGCTGCTATTTC; NHE3-F CACCACAGGATTGTCCCTCT; NHE3-R: ACAGCAGGAAGGCGAAGATA; NHE4-F: GGCTTTCTCCTGAAGACGTG; NHE4-R: GTCTGTCGCCTTTCCTGAAG; NHE5-F: GCTGAGGGTGAAGAGGAGTG; NHE5-R GGCATAGAGGGCAGAGTGAG.

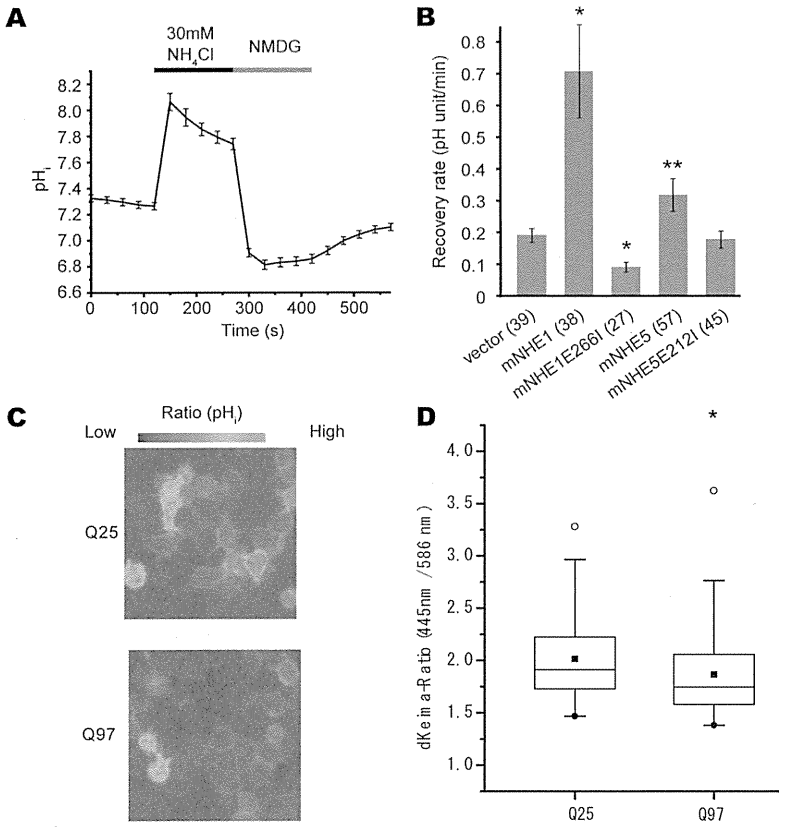

Figure 1. Acidification by polyglutamine protein expression visualized by dKeima-mem-based subcellular pH imaging. A. Representative subcellular pH imaging data in Neuro-2a cells expressing dKeima-mem during acidification followed by recovery in Na^+-free and Na^+-containing medium. B. Expression of NHE1 and NHE5 but not by their non-functional mutants facilitates recovery from acidification (see Methods). Mean pH recovery rate ±SD for each type of cells is shown as a bar graph. *P<0.01, **P<0.05 (Student's t-test; in comparison with the recovery rate of vector-only transfected control cells). Numbers in parentheses on X axis indicates the number of cells examined. C, D. Representative intracellular pH imaging results of Neuro-2a cells expressing dKeima-mem together with HttEx1-Q25 or HttEx1-Q97 demonstrated by pseudo-color images (C) and box whisker plot of quantification data 445 nm/586 nm emission ratio(D). In D, boxes represent lower quartile and upper quartile, with bars showing 1.5× of the lower and upper quartile values. White and black circles show max and min, respectively, and quadrangles show median data points. *P<0.001 (Welch's t test).
doi:10.1371/journal.pone.0081313.g001

Results

Change in extracellular pH induces autophagosome formation in the Neuro-2a cells stably expressing EGFP-LC3

Previous reports suggested that autophagy in neuronal cells is regulated in a way different from non-neuronal cells [15]. To gain insights on the mechanism of macroautophagy induction in neuron-like cells, we generated mouse neuroblastoma-derived Neuro-2a cells stably expressing EGFP-LC3 and used them as a neuron-like model system. Among physiologically relevant neuronal environmental changes that affect intracellular protein degradation, we chose to examine the effect of environmental pH changes on neuronal autophagy, because lysosomal protein degradation is heavily dependent on cellular pH regulation [16]. To modify environmental pH in cultured cells, we examined Neuro-2a cells stably expressing EGFP-LC3 maintained in an incubator with 100% air (no added CO_2) for 2 hr. We found that numbers of EGFP-positive spots were significantly increased by incubating the cells under normal air, while EGFP spot formation was not significantly affected by serum deprivation using DMEM lacking serum as culture media (FBS(−)) or by serum/amino acid-deprivation using Krebs-Ringer bicarbonate solution (KRB)(Fig. 2A). This result suggested that pH of culture environment of Neuro-2a cells affects autophagosome formation in them.

To gain insights on the mechanism of this phenomenon, we first tried to analyze which ion channels or transporters are functional in Neuro-2a cells. Major transporters implicated in intracellular pH regulation in various types of cells include sodium-hydrogen exchangers (NHEs/ SLC9 gene family) and several members of bicarbonate transporter superfamily of molecules [17]. Previous reports showed that all the known isoforms of bicarbonate-dependent transporters are inhibited by diisothiocyanostilbene disulfonic acid (DIDS) [18], while members of NHE family are inhibited by 5-(N-ethyl-N-isopropyl)-amiloride (EIPA) [19]. Therefore, we first tried these inhibitors on the Neuro-2a cells. We found that application of EIPA to the Neuro-2a cells in a 5% CO2 incubator significantly increased formation of EGFP-positive spots in the cells, while DIDS showed no effects (Fig. 2B). This result suggested that NHEs play a role in autophagosome formation in

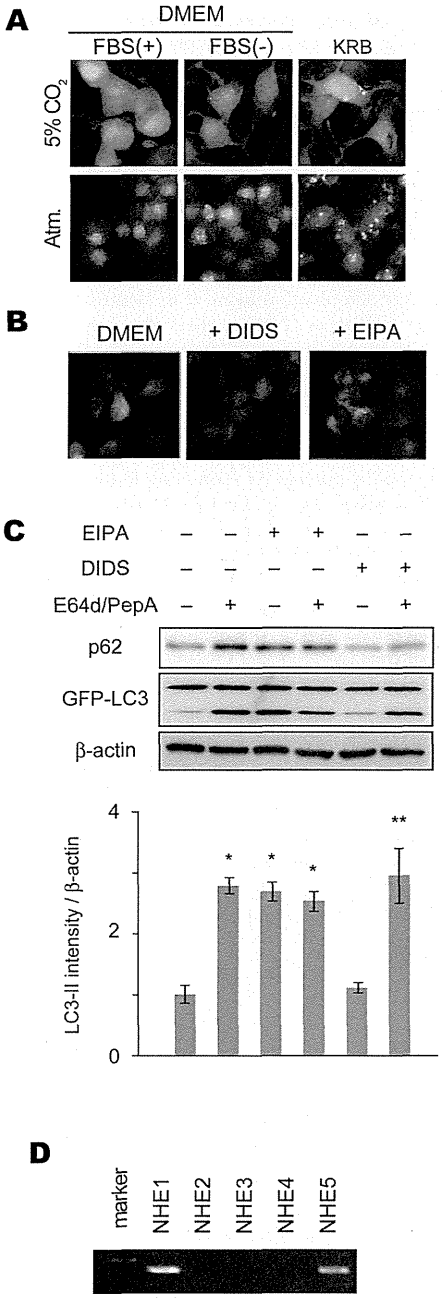

Figure 2. Neuro-2a cells show increased autophagosome formation in response to environmental pH modulation. A, B Representative photomicrographs of Neuro-2a cells stably expressing EGFP-LC3 maintained under indicated medium and atmosphere conditions for 2 hr (A), or with indicated reagents in serum-containing DMEM under 5% CO2 (B). Note the significantly increased autophagosome formation in the cells maintained in Krebs-Ringer bicarbonate buffer (KRB), which contains electrolites and glucose only under 100% normal air, and with EIPA. C Representative images of immunoblot analysis for expression of p62 and LC3 in EGFP-LC3-expressing Neuro-2a cells with indicated reagents. Bar graphs in C show quantification data of LC3-II expression levels relative to the level in EGFP-LC3-expressing Neuro-2a cells with no additional treatment normalized to β-actin expression. Results shown are mean ± SEM. *P<0.01, **P<0.05 (Student's t- test). Note that EIPA-treated cells show increased p62 and LC3-II levels indicating the inhibition of autophagic degradation by NHE inhibition. D. Detection of NHE family members in Neuro-2a cells by RT-PCR.
doi:10.1371/journal.pone.0081313.g002

the Neuro-2a cells. To distinguish whether EIPA-induced induction of autophagosome formation in Neuro-2a cells is involved in lysosomal acidification only or in induction of autophagy as well, we first performed autophagy flux assays in the presence of EIPA or DIDS (used as a negative control) [20]. We examined expression levels of p62 and LC3-I/II in Neuro-2a cells expressing GFP-LC3 in the presence of EIPA or DIDS, before and after lysosomal inhibitor (E64d/PepA) treatment. We found that EIPA treatment increased both p62 and LC3-II levels, suggesting that EIPA inhibited basal levels of autophagy in Neuro-2a cells, while DIDS did not affect the autophagy level (Fig. 2C). These results suggest that NHEs may affect autophagy levels in Neuro-2a cells. We then examined which family members of NHEs are expressed in Neuro-2a cells by RT-PCR, and found that NHE1 and NHE5 mRNA were detectable, while other members were not (Fig. 2D).

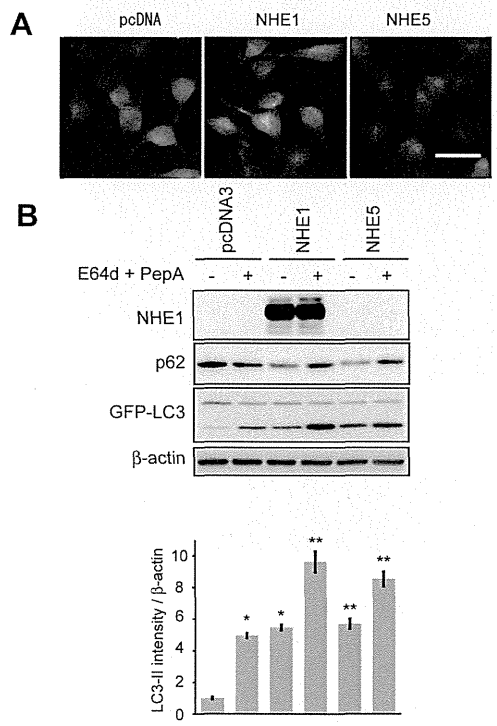

Figure 3. Induction of autophagy in Neuro-2a cells by NHE1 and NHE5. Representative photomicrographs of Neuro-2a cells stably expressing EGFP-LC3 with additional expression of NHE1 or NHE5 (A). Scale bar = 50 μm. Representative images of immunoblot analysis for expression of p62 and LC3 in EGFP-LC3-expressing Neuro-2a cells overexpressing indicated constructs (B). Bar graphs in B show quantification data of LC3-II expression levels relative to the level in EGFP-LC3-expressing Neuro-2a cells with no additional treatment normalized to β-actin expression. Results shown are mean ± SEM. *P<0.01, **P<0.05 (Student's t- test). Note that induced levels of LC3-II by overexpression of NHE1 and NHE5 was further increased by E64d/PepA, suggesting that expression of NHE1 and NHE5 induces autophagy in B.
doi:10.1371/journal.pone.0081313.g003